Atmospheric Research 308 (2024) 107545

Contents lists available at ScienceDirect

Atmospheric Research

journal homepage: www.elsevier.com/locate/atmosres

Large-scale dynamic processes during the minor and major sudden stratospheric warming events in January–February 2023

P.N. Vargin [a,b,*], A.V. Koval [c,d,**], V.V. Guryanov [e], B.M. Kirushov [a]

[a] Central Aerological Observatory, 141700 Dolgoprudny, Moscow Region, Russia
[b] Obukhov Institute of Atmospheric Physics of the Russian Academy of Science, 119071 Moscow, Russia
[c] Atmospheric Physics Department, Saint Petersburg University, 199034 Saint Petersburg, Russia
[d] Ozone Layer and Upper Atmosphere Research Laboratory, Saint Petersburg University, 199034 Saint Petersburg, Russia
[e] Kazan Federal University, 420008 Kazan, Russia

ARTICLE INFO

Keywords:
Stratosphere
Sudden stratospheric warming
Planetary waves
Residual meridional circulation
Ozone layer
Ozone mini hole

ABSTRACT

Using data from reanalyses of meteorological information, this study examines peculiarities of the thermodynamic regime of the Arctic stratosphere in the winter season of 2022–2023. For this purpose, components of the global meridional circulation, wave activity fluxes, volume of polar stratospheric clouds type I (PSC NAT) are analyzed, as well as changes in these indicators during sudden stratospheric warming (SSW) events formed in January–February. The main features of the 2022–2023 winter season were the following: (1) a persistent cold stratospheric polar vortex was observed until mid-January, which caused the PSC NAT volume growth to its maximum values since 1980; (2) enhanced wave activity from mid-January led to the formation of a minor SSW at the end of January, an increase in the temperature of the lower stratosphere and a sharp reduction in PSC NAT; (3) a week of intensification of the polar vortex was then observed, followed by a weakening due to the next burst of wave activity propagation during the second SSW event in mid-February. This second SSW event was major, accompanied by a reversal of the mean zonal wind, which lasted until early March; (4) meridional heat flux in January–February 2023 was the highest since 1948, resulting in unprecedented warming of the lower Arctic stratosphere and preventing ozone depletion in March; (5) the minor SSW at the end of January was accompanied by a more intense change in the meridional circulation than the major SSW in mid-February. Formation of ozone mini-hole over Northern and Central Europe in February 2023 was associated with the strengthening of the anticyclone, leading to a stratopause elevation and northward transport of ozone-poor air masses from the subtropics along the western periphery of the anticyclone additionally to related to the major SSW temperature changes affected the ozone concentration in the lower stratosphere.

1. Introduction

The main factor determining the thermodynamic regime in the boreal winter stratosphere is the interaction of a stratospheric polar vortex and planetary waves. The polar vortex is formed during polar night conditions due to enhancement of the meridional thermal gradient at middle and high latitudes. A change in the intensity of the polar vortex in winter is associated with the momentum exchange between the mean flow and waves, which structure is also subject to strong variability.

Sudden stratospheric warming (SSW) is one of the most important and attractive events of the winter season and characterized by the polar vortex weakening, polar stratosphere temperature increase by tens of degrees, deceleration of mean flow and its reversal at 10 hPa and 60° N in the case of the major SSW (Matsuno, 1971; Baldwin et al., 2021; Butchart, 2022). For unknown reasons SSW did not observe in several years during some periods but later they occurred every winter (Manney et al., 2005). Notably that some SSW events do not satisfy the conditions of major SSW, nevertheless they may have a significant and long-lasting impact on the Arctic stratosphere (Manney et al., 2015). Simultaneously with polar stratosphere temperature increase during the SSW the meridional circulation intensifies including descending branch strengthening in the subpolar stratosphere, which in turn leads to its warming (Koval et al., 2021).

* Correspondence to: Vargin P.N., Central Aerological Observatory, 141700 Dolgoprudny, Moscow Region, Russia.
** Correspondence to: Koval A.V., Atmospheric Physics Department, Saint Petersburg University, 199034 Saint Petersburg, Russia.
E-mail addresses: p_vargin@mail.ru (P.N. Vargin), a.v.koval@spbu.ru (A.V. Koval).

https://doi.org/10.1016/j.atmosres.2024.107545
Received 26 January 2024; Received in revised form 21 June 2024; Accepted 23 June 2024
Available online 24 June 2024

Strengthening of planetary wave propagation from the troposphere into the stratosphere and planetary waves interaction with the mean flow are responsible for the SSW formation (Matsuno, 1971; Baldwin et al., 2021; Butchart, 2022). However, according to model simulations some SSW events may occur due to internal stratospheric oscillations (e.g., Pogoreltsev et al., 2015; Baldwin et al., 2019).

In the absence of SSW, the temperature of polar stratosphere decreases and may exceed the threshold of formation of polar stratospheric clouds (PSC) playing a critical role in ozone depletion in late winter and spring. PSCs are composed predominately of crystalline nitric acid trihydrate (PSC NAT type I). PSCs provide medium for the conversion of inert reservoir species like HCl, HBr, and $ClONO_2$ to Cl_2, BrCl, and $ClNO_2$ that are later transformed into active forms in the presence of solar irradiance (Solomon et al., 1986) leading to springtime ozone depletion induced by catalytic cycles. PSCs are also responsible for the removal of nitric acid compounds from the lower polar stratosphere as a result of settling ("denitrification"), which is capable of neutralizing active and dangerous for the ozone layer chlorine atoms. Therefore, the larger and long-lasting PSC volume in late winter corresponds to stronger ozone layer depletion. Over the all years of observations the strongest ozone layer depletion in the Arctic stratosphere occurred in the winter 2019–2020 (Lawrence et al., 2020; Wohltmann et al., 2021; Smyshlyaev et al., 2021; Tsvetkova et al., 2021).

Analysis of observational and modeling data show that as a result of the SSW, the probability of winter cold spells in some regions including Northern Europe and Eastern Siberia increase by 40%–50% (Kolstad et al., 2010; Tripathi et al., 2015). This cold spells formation particularly over Northern America may be related to prior downward refraction of planetary waves from the stratosphere into the troposphere (Kodera et al., 2008; Nath et al., 2016; Matthias and Kretschmer, 2020).

Changes of circulation and temperature associated with SSW penetrate into the upper atmosphere. Particularly, the mesosphere temperature decreases, circulation direction changes, and stratopause height descends (Baldwin et al., 2019; Gasperini et al., 2023). After major SSW with prolonged zonal wind reversal, a new "elevated" stratopause may be formed in the lower mesosphere, which slowly descends to its climatological winter height. This stratopause displacement was named "Elevated Stratopause Event" (ESE) and was first described on the basis of the rocket data analysis of the 1971–1972 winter (Labitzke, 1972). In the equatorial ionosphere the electron density perturbations caused by SSW may be comparable in amplitude with those caused by moderate geomagnetic storms (e.g., Goncharenko et al., 2010; Klimenko et al., 2015).

Due to differences in the formation processes, strength, timing of formation and persistence, deterministic predictability of SSW events is limited to 10–15 days with rare exceptions (e.g., Karpechko et al., 2018; Rao et al., 2019; Tsvetkova et al., 2020). Moreover, their magnitude is generally underestimated in sub-seasonal prediction models (e.g., Karpechko et al., 2018; Lawrence et al., 2022). As far as SSWs substantially determine the interseasonal and interannual variability of Arctic stratosphere, a better understanding of dynamic processes responsible on these events onset and persistence is necessary for weather forecast improvement (Tian et al., 2023). Despite decades of research after SSW discovery (Scherhag, 1952) many aspects on the mechanisms driving SSWs and defining its strength, duration, impacts on circulation of troposphere and stratosphere, circulation and chemical content of the upper atmosphere are not fully understood. Most review articles that attempt to systematize sudden stratospheric warmings (SSWs) (Butler et al., 2015) or obtain any statistical characteristics of events (Zhang et al., 2021) are written on the basis of detailed analyzes of information of each SSW occurring in Arctic on average twice every three years. The development of SSW forecasting (de Fondeville et al., 2023; Rupp et al., 2023) and approaches for its monitoring (Li et al., 2023) are also based on the studies in which the temperature anomaly, reversal of zonal wind, the behavior of the stratospheric polar vortex, as well as a number of other characteristics (e.g., Baldwin et al., 2021) were obtained and analyzed for every single SSW event. Therefore, every winter season in the Arctic stratosphere is interesting and relevant to the investigation (e.g., Roy and Kuttippurath, 2022; Vargin et al., 2022).

Due to formation of minor SSW in late January and major SSW in mid-February with long-lasting effects on stratosphere, ozone layer, and troposphere, the 2022–2023 winter season needs to be studied as an interesting example of interseasonal and interannual variability of Arctic stratosphere. To date, two publications have been dedicated to the analysis of the atmospheric dynamics during this winter. First study is focused on stratosphere-troposphere dynamical coupling (Lu et al., 2023). Particularly, the authors show that short weakening of the stratospheric polar vortex in early December 2022 was followed by large cold anomalies occurred in the Eurasian continent and later in North America. The authors suggest that multiply weakening of Arctic stratospheric polar vortex in the 2022–2023 winter was accompanied by severe loss of Barents-Laptev Sea ice and anomalously cold tropical Pacific sea surface temperatures (La Niña), which have been reported to be conducive to the enhancement of planetary waves 1 and 2 respectively. Additionally, two weeks before the major SSW, Madden - Julian oscillation developed into phases 4–6, also contributing to the occurrence of this event. Second study investigates the SSW impacts on ozone layer (Mukhtarov et al., 2023). It was shown that increase in total ozone content (TOC) in Arctic during the SSW events was caused by increase in ozone concentrations in the lower stratosphere. The authors revealed a relationship between sharp TOC changes particularly nearby Sofia (42° N, 24° E) from ~450 DU to ~250 DU in February 2023 and temperature changes related to the major SSW characterized by positive correlation (above 0.5) in the lower stratosphere nearby the altitude of ozone concentration maximums.

Present study aims to investigate large-scale dynamic processes related to formation of the minor SSW in late January and the major SSW in mid-February 2023 and impacts of these events on the stratosphere, troposphere, and ozone layer. The paper is organized as follows: Section 2 describes employed data and methods of analysis. Obtained results on large-scale dynamic processes in extratropical northern stratosphere in the 2022–2023 winter, including wave activity, residual mean meridional circulation, formation of the minor and major SSW events in late January and in mid-February respectively, stratopause displacement associated with these SSWs, impacts of the polar stratosphere variability on the troposphere, ozone layer, and formation of ozone mini hole over Northern and Eastern Europe during the major SSW onset are described in Section 3. Conclusions are given in Section 4.

2. Data and methods

Large-scale dynamic processes of the Arctic stratosphere in the 2022–2023 winter were analyzed using reanalysis data of NCEP (Kalnay et al., 1996), ERA5 (Hersbach et al., 2020), and MERRA-2 (Gelaro et al., 2017). A good agreement among reanalyses for dynamical processes related to SSW events, including triggering mechanisms, tropospheric precursors, and surface response was shown (Ayarzaguena et al., 2019). The NCEP and ERA5 reanalysis data anomalies were calculated relative to the climate means averaged over the time interval from 1981 to 2010, and the MERRA-2 reanalysis from 2004 to 2023.

To investigate stratospheric circulation and wave - mean flow interactions associated with the SSW events amplitudes of dominant in the extratropical stratosphere planetary waves with zonal wave numbers 1–3, zonal-mean meridional heat flux $\overline{v'T'}$ (denoted further as *HF)*, where v' and T' are deviations from the zonal-mean values of meridional wind and temperature, and 3-dimensional Plumb flux (Plumb, 1985) were calculated. Under the assumption of slow variability of the basic state (WKB limit), the Plumb flux vectors are proportional to the group velocity of a planetary wave packet indicating the direction of propagation of the wave activity. Data averages over 3 days were used in the calculation of the Plumb flux vectors in the periods of SSWs formation

characterized by fast changes of wave activity, temperature, zonal wind and etc. When averaged over longitude, Plumb flux corresponds to the Eliassen-Palm flux (Andrews et al., 1987).

Downward propagation the reflected planetary wave activity flux was assessed using approach developed by Perlwitz and Harnik (2004). It represents calculation of reflective index as a difference in the zonal mean wind speed in the latitudinal belt of 58° N - 74° N between the layers of 2 hPa and 10 hPa. The positive values of this reflective index denote unfavorable conditions for reflecting wave activity flux. Residual meridional circulation (RMC) within the Transformed Eulerian Mean approach (TEM, Andrews et al., 1987) was calculated using MERRA-2 reanalysis data. The RMC calculation is a convenient method for analyzing the interaction of waves with the mean flow. Definition and concept of the RMC was discussed in details by Koval et al. (2021).

Volume of the air masses in the lower stratosphere within the stratospheric polar vortex with temperatures sufficient to form a PSC NAT I-type (hereafter Vpsc) is often used as an indicator of favorable conditions to severe ozone loss. To analyze intraseasonal variability of such conditions, the Vpsc estimates provided by Ozone Watch project (*NASA Ozone Watch*, 2024) were used. These estimates were calculated according to Lawrence et al. (2018) using MERRA-2 reanalysis data.

The associated with SSWs changes in the stratopause height in Arctic were analyzed using data with an upper boundary is at 0.0003 hPa (~106 km) from the MLS instrument installed on the Aura satellite (Waters et al., 2006). Employed assimilation procedure of MLS data is described in Vargin and Kiryushov (2019).

Time evolution of the Northern Annular Mode (NAM) index from the middle stratosphere (10 hPa) down to the surface was analyzed as an indicator of the stratosphere-troposphere dynamical coupling. This index was calculated as daily geopotential height anomalies normalized to the standard deviation in the latitudinal belt of 65° N - 90° N and multiplied by (−1) to match the Arctic Oscillation index.

Described above analyses are aimed to reveal peculiarities of large-scale dynamical processes in the Arctic stratosphere winter 2022–2023 with the focus on its most disturbed period January–February with two minor SSWs and one major SSW and to investigated influence of these processes on the circulation of stratosphere, stratosphere-troposphere dynamical coupling, and the ozone layer.

Finally, to analyze ozone mini-hole formed over Northern and Eastern Europe in mid-February 2023, the ERA5 reanalysis data of total ozone content and potential vorticity at isentropic levels were used.

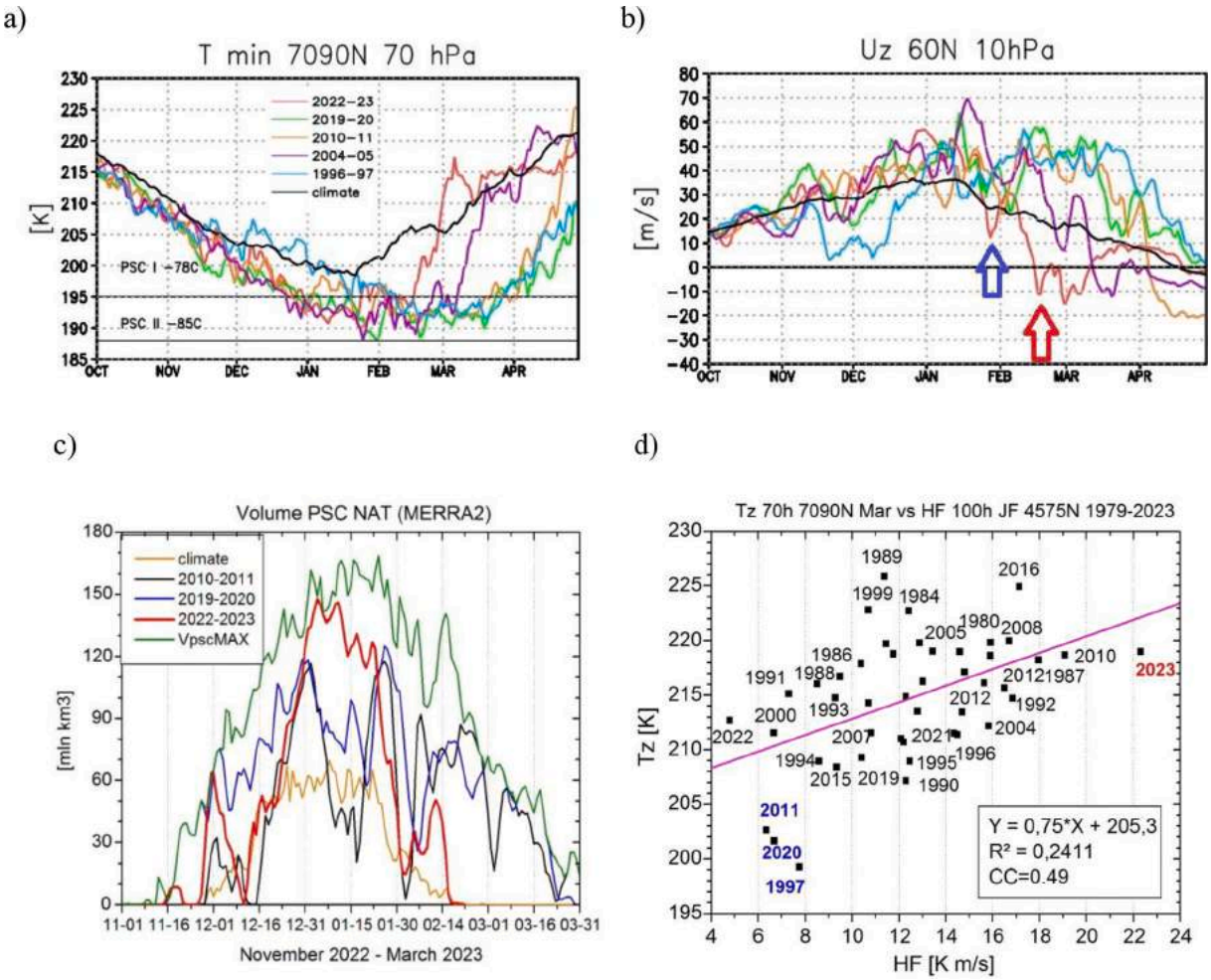

Fig. 1. Minimum temperature averaged over 70° N - 90° N at 70 hPa (~ 16 km) (a), zonal mean wind at 60° N and 10 hPa (~30 km) from October to April for the winter seasons: 1996–1997, 2004–2005, 2010–2011, 2019–2020, 2022–2023, and climate mean (1978–2022). Blue arrow indicates minor SSW, red arrow - major SSW (b). V_{PSC} from November to March of winter seasons of 2010–2011, 2019–2020, 2022–2023, and climate mean and maximum values over the period of 1978–2022 (c). Scatter diagram of lower stratosphere temperature mean 70° N - 90° N at 70 hPa in March vs zonal mean heat flux 45°N -75° N mean at 100 hPa in January–February from 1979 to 2023. Three March months with the lowest temperature (1997, 2011, 2020) and March 2023 with the largest HF are marked by blue and red colors respectively (d). (For interpretation of the references to colour in this figure legend, the reader is referred to the web version of this article.)

3. Results

3.1. Main features of the winter 2022–2023

The 2022–2023 winter was the third consecutive warm season in the Arctic stratosphere after the coldest winter 2019–2020, when the most stable and longest-lasting polar vortex was observed (persisted untill March), contributing to unprecedented ozone depletion (Lawrence et al., 2020; Wohltmann et al., 2021; Smyshlyaev et al., 2021; Tsvetkova et al., 2021). The 2022–2023 winter season is an example of high intraseasonal variability in the polar stratospheric circulation: it was characterized by a strong and cold stratospheric polar vortex existed until the end of January. The lower polar stratosphere minimum temperature describing the conditions for PSC formation inside the polar vortex as well as zonal-mean zonal wind speed (hereafter referred to as zonal wind speed) in the middle stratosphere at 10 hPa were comparable to those during the 2019–2020 winter season (Fig. 1a and b).

In December 2022 the zonal wind speed in the middle stratosphere at pressure level of 10 hPa and 60° N, except for short lasting weakening at the beginning (Lu et al., 2023), was close to climatic means till the end of the month (Fig. 1b). Then the strengthening of zonal wind began and by the late December - early January its speed exceeded climate mean values by ~20 m/s and became comparable to the values of the 2019–2020 winter.

During the minor SSW in late January, the zonal mean wind at 10 hPa and 60°N weakened sharply from ~45 m/s, which is ~15 m/s greater than climate values, to ~10 m/s, which is less than climate values. After a short amplification in the beginning of the February, the zonal wind weakened and on February 16 its reversal was observed corresponding to the major SSW event. This zonal wind reversal was observed over 3–4 days from ~25 km up to about 60 km with the maximum nearby 45 km (Fig. A10a). Subsequently, the zonal wind strengthened up to 30–40 m/s in the upper stratosphere whereas its values did not exceed 10 m/s in the lower stratosphere till spring break up in mid-April.

Since early December, Arctic lower stratosphere temperature has decreased to threshold values at which PSC formation is possible (Fig. 1a). From mid-December, a rapid increase in the PSC NAT volume (V_{PSC}) was observed: by the early January, when the largest negative temperature anomalies of the polar lower stratosphere reached up to −10 K, a maximum V_{PSC} of ~140 mln. km^3 was observed, which was comparable to the maximum values over all years of observations and higher than the values of the winter 2019–2020 by ~30 mln. km^3 (~20%) (Fig. 1c). During the minor SSW in late January, the V_{PSC} decreased sharply from ~120 mln km^3 in mid-January to ~20 mln km^3.

An interesting peculiarity of the 2022–2023 winter season was the highest value of the zonal mean meridional heat flux (*HF*) in the lower stratosphere at a pressure level of 100 hPa, characterizing the propagation of wave activity into the middle and upper polar stratosphere, in January–February among all winter seasons since 1979 (Fig. 1d). This parameter is known to be related to the temperature of the lower polar stratosphere in March, when the strongest ozone depletion is observed (Newman et al., 2001). When considered using NCEP reanalysis data since 1979, the correlation coefficient (CC) between these parameters is 0.49. The CC is significant according to Student's *t*-test at a significance level of 0.99. The January–February 2023 *HF* value is also the largest in the longer time series since 1948, but the *CC* drops to 0.27 (Fig. A10b). It can be assumed that the decrease of the *CC* may be caused particularly by differences in interseasonal variability of the wave activity propagation in the pre-satellite era.

The polar lower stratosphere temperature, as discussed earlier, was below climatic values by 5–10 K in the lower stratosphere and up to 15–20 K in the upper stratosphere until mid-January 2023. Simultaneously, from the middle of January, the downward propagation of positive temperature anomalies from the upper stratosphere to the lower stratosphere was observed. By the end of January in the lower stratosphere, these anomalies reached up to 15–20 K (Fig. 2a). During the same period corresponding to the minor SSW, the positive zonal wind speed anomalies at 60° N decreased from 30 to 40 m/s almost to zero (Fig. 2b). In the middle of February during the major SSW, the positive temperature anomalies reached up to 35 K, the zonal wind speed became slower than the climatic values by 10–20 m/s in the lower stratosphere and by 70–80 m/s in the upper stratosphere. The zonal mean wind anomalies from the climatic values in February are shown with shading in Fig. 2c. The major SSW caused a significant weakening of the stratospheric polar vortex. Interestingly that in the upper stratosphere the polar vortex recovered shortly after the major SSW.

As a result of the minor SSW, the minimum temperature of the Arctic lower stratosphere increased by ~5 K and for the first time since the late December 2022 exceeded the threshold values for the formation of PSC NAT type 1. The polar stratospheric temperature anomalies at the end of January became positive for the first time during the winter season 2022–2023: up to ~5 K in the lower and up to ~10 K in the middle polar stratosphere.

3.2. Wave activity

The minor SSW at the end of January was accompanied by the maximum for the winter season increase in the planetary wave amplitude with zonal number 1 (hereinafter referred to as wave 1) up to ~550 gpm in the lower stratosphere (70 hPa) and up to ~1700 gpm in the middle stratosphere (10 hPa) over the high latitudes. After a small weakening in early February during the development of the major SSW, the strengthening of the wave 1 amplitude up to ~450 gpm in the lower stratosphere (70 hPa) and up to ~1400 gpm in the middle stratosphere (10 hPa) of high latitudes was observed. Hence, both the minor SSW and the major SSW events were characterized by the intensification of wave 1 and the displacement of the stratospheric polar vortex in the middle and lower stratosphere from the pole.

The amplitude of wave 2 was 3–5 times less than wave 1 amplitude in the middle stratosphere during the minor and major SSW events (Fig. 3a). In the lower stratosphere the largest amplitudes of wave 2 were observed in January and in early February, but amplitude of wave 2 was comparable with the amplitude of wave 1 only during three 1–3 days intervals (Fig. 3b). In the upper troposphere amplitudes of wave 1 and wave 2 from early January to late February were comparable (Fig. 3c).

The zonal mean heat flux (*HF*) in the lower stratosphere in the region of 50° N - 60° N after the period from mid-December to mid-January, when its values did not exceed ~20 K m/s, intensified to ~60 K m/s around January 20 during the period of minor SSW (Fig. 3d). A few days later, an area of *HF* negative values is formed at high latitudes for about 7 days, indicating the reflection of wave activity to the troposphere. The next two periods of heat flux intensification in the lower stratosphere with a maximum near 60° N and 75° N were observed around February 15 before the major SSW and at the end of February, respectively.

After the strengthening in early December a long-lasting weakening of *HF* was observed from mid-December to mid-January from the upper troposphere to the stratosphere (Fig. 3e). Afterwards there were three periods of its strengthening: in middle and late January and in mid-February.

A short-term weakening of the stratospheric polar vortex in early December 2022 revealed by Lu et al. (2023) was accompanied by an increase in the propagation of wave activity into the stratosphere and an intensification of the planetary wave with zonal number 1 (Fig. 3c) and 3 (not shown) in the upper troposphere and lower stratosphere.

3.3. Change in residual mean meridional circulation

To study changes in RMC during both SSWs, 7-day time intervals before and during the SSW were selected. Altitude-latitude distributions of anomalies of RMC components and temperature relative to the

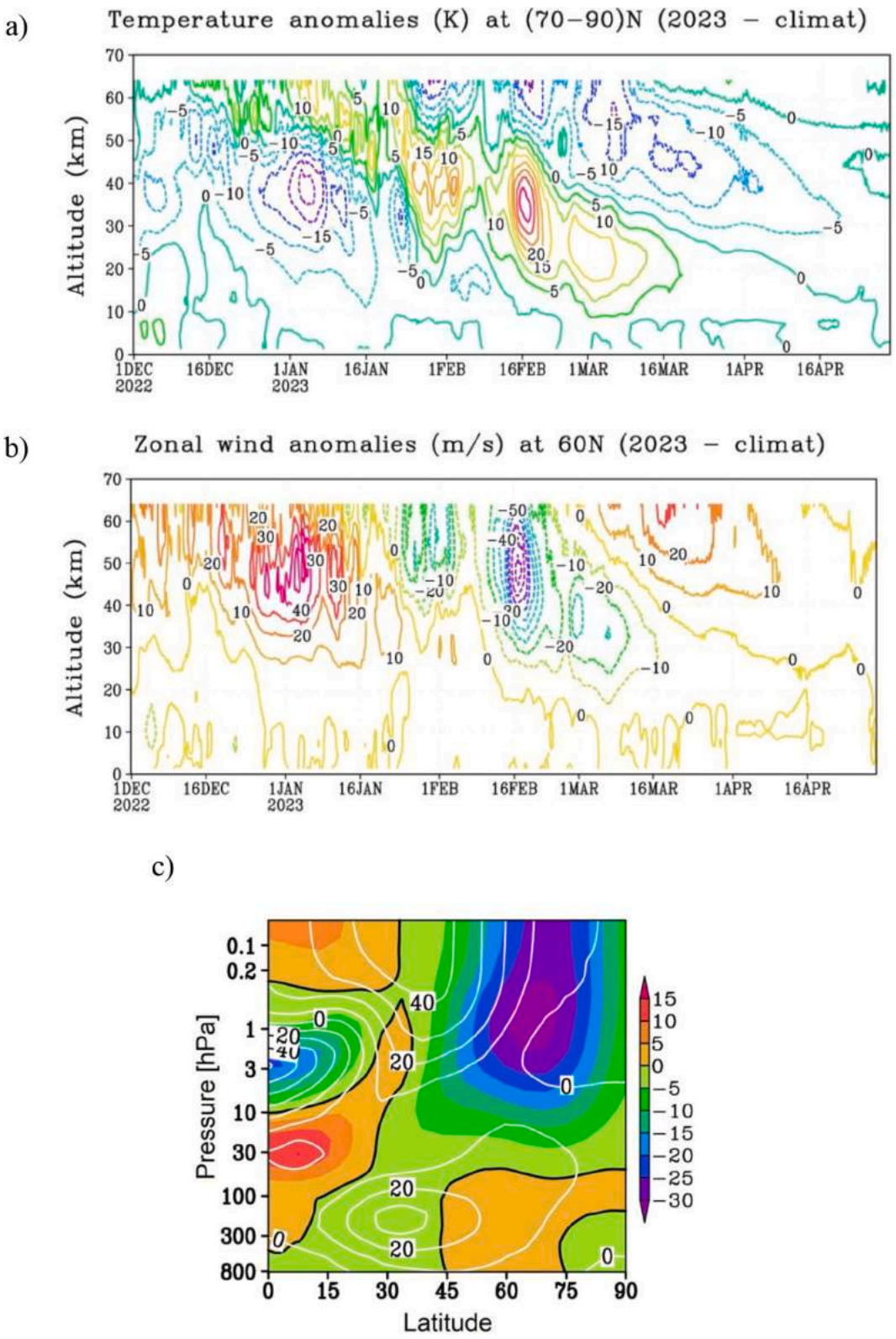

Fig. 2. Temperature anomalies mean 70° N - 90° N (a) and zonal wind speed at 60° N (b) from December 1, 2022 to April 30, 2023 relative to climate mean (2004–2023). Zonal wind in February 2023 (contours) and its anomalies from climate mean (shading) respectively (c).

climate average for 20 years (from 2004 to 2023) before the minor SSW and during the event are shown in Figs. 4a-b. Fig. 4c demonstrates the difference in RMC and temperature between the intervals before and during the SSW.

The subpolar region below 3 hPa is colder than the climatic value before the SSW (Fig. 4a). This is explained by the fact that the polar vortex by this time (by January 16) began to weaken, but is still stronger than normal (climatic), and the wave activity fluxes in the lower stratosphere, on the contrary, are weakened, which leads to a weakening of the meridional heat flux on the eve of the minor SSW. In addition, the

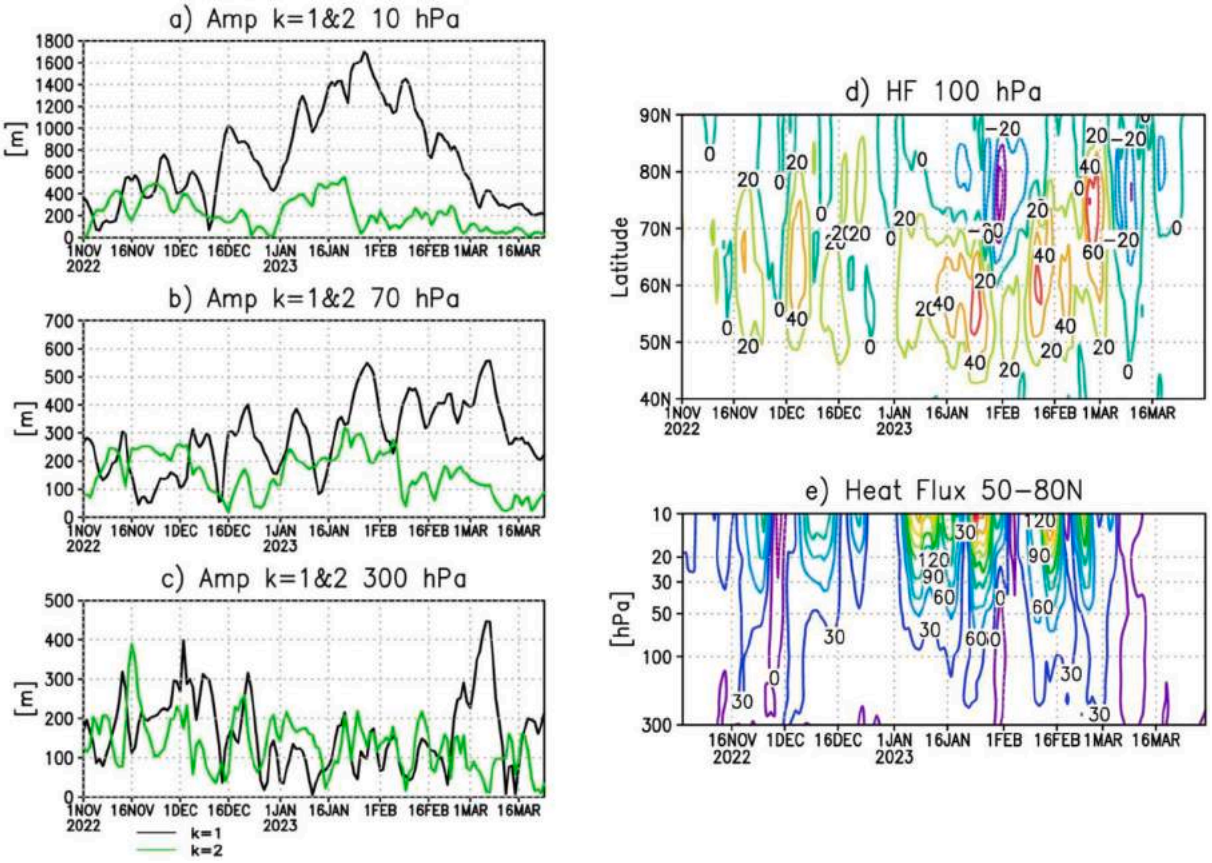

Fig. 3. Amplitude of planetary waves with zonal number 1 and 2 (gpm) averaged over 45° N -75° N at pressure levels of 10 hPa, 70 hPa, and 300 hPa (a, b, c); zonal mean heat flux *HF* (K m/s) at 100 hPa in the latitudinal belt from 40° N to 90° N (d) and averaged over 50° N - 80° N for upper troposphere - lower stratosphere (300 hPa–10 hPa) from November 1, 2022 to March 30, 2023 (e).

weakening of the descending branch of the RMC (the anomaly arrows are directed upwards), associated precisely with the weakening of wave activity and, consequently, with the weakening of the eddy component of the RMC, causes adiabatic cooling. Above the level of 3 hPa, wave activity intensifies, poleward heat fluxes also intensify, and the eddy component of the RMC enhances the meridional (poleward and downward) transport. The heating process of the polar region gradually starts, which, with further intensification of wave activity, leads to the formation of a minor SSW. The SSW time interval is shown in Fig. 4b. Starting from the low-latitude stratosphere, acceleration of the meridional component of the RMC is observed. In the mid- and high-latitude stratosphere (up to a pressure level of 1 hPa), the RMC further intensifies. The polar vortex weakens and intense heating occurs. The strengthening of the meridional branch of the RMC at middle latitudes also leads to the formation of ascending flows, cooling and lowering of the stratopause. Such heating/cooling processes in the polar stratomesosphere lead to downward displacement of the stratopause (see section 3.6) during the minor SSW and lasting till the major SSW. Circulation changes during a minor SSW are clearly visible in Fig. 4c.

Fig. 4d shows temperature and RMC anomalies relative to climate in the time interval between two SSWs. The circulation did not recover to climate conditions after the first SSW, the ascending wave activity weakened after the first SSW, but remains reinforced, this explains the continued heating of the subpolar region and the increments in the RMC velocity. It is interesting that during the major SSW, despite the reversal of the zonal flow, after February 16 (Fig. 4e), there is no further strengthening of the RMC in the high-latitude stratosphere, as usually occurs during the SSW (e.g., Koval et al., 2021). This is clearly visible in Fig. 4f, where only a slight increase in the downward component of the RMC is observed at 80° N during the major SSW. A significant increase in temperature (up to 25 K) is explained by an increase in wave activity and, accordingly, meridional heat fluxes.

As a result, the temperature anomaly relative to climate, as would be expected, is larger during the major SSW in February than during the minor SSW at the end of January, but the RMC anomalies during the minor SSW are stronger. If we consider the anomalies of these parameters during a SSW relative to the situation before the event, then the minor SSW causes a more substantial change in circulation and is accompanied by greater changes in wave activity fluxes than the major SSW.

3.4. Minor SSW at the end of January 2023

In this section, when analyzing fast changes of wave activity during the period of SSW in the troposphere and lower stratosphere using Plumb vectors, 3-day time intervals were considered in contrast to the RMC analysis in the previous section, where 7-day time intervals were selected in order to illustrate the changes of the RMC main large-scale features in the upper stratosphere. To study the peculiarities of the propagation of planetary waves during the period of SSW formation, the Plumb vector distribution diagrams were plotted (Fig. 5).

During the period of the minor SSW onset at the end of January, an increase of the wave activity fluxes propagating from the troposphere to the stratosphere was observed, which resulted in weakening of the zonal wind, for example, near the pressure level of 10 hPa and 60°N from ~45 m/s to ~20 m/s (Fig. 5a, b). At the same time, the reflection of wave activity fluxes into the troposphere from the stratosphere in the region of 70° N - 80° N began (Fig. 5b).

The minor SSW was accompanied by the increased propagation of wave activity from the troposphere to the stratosphere over

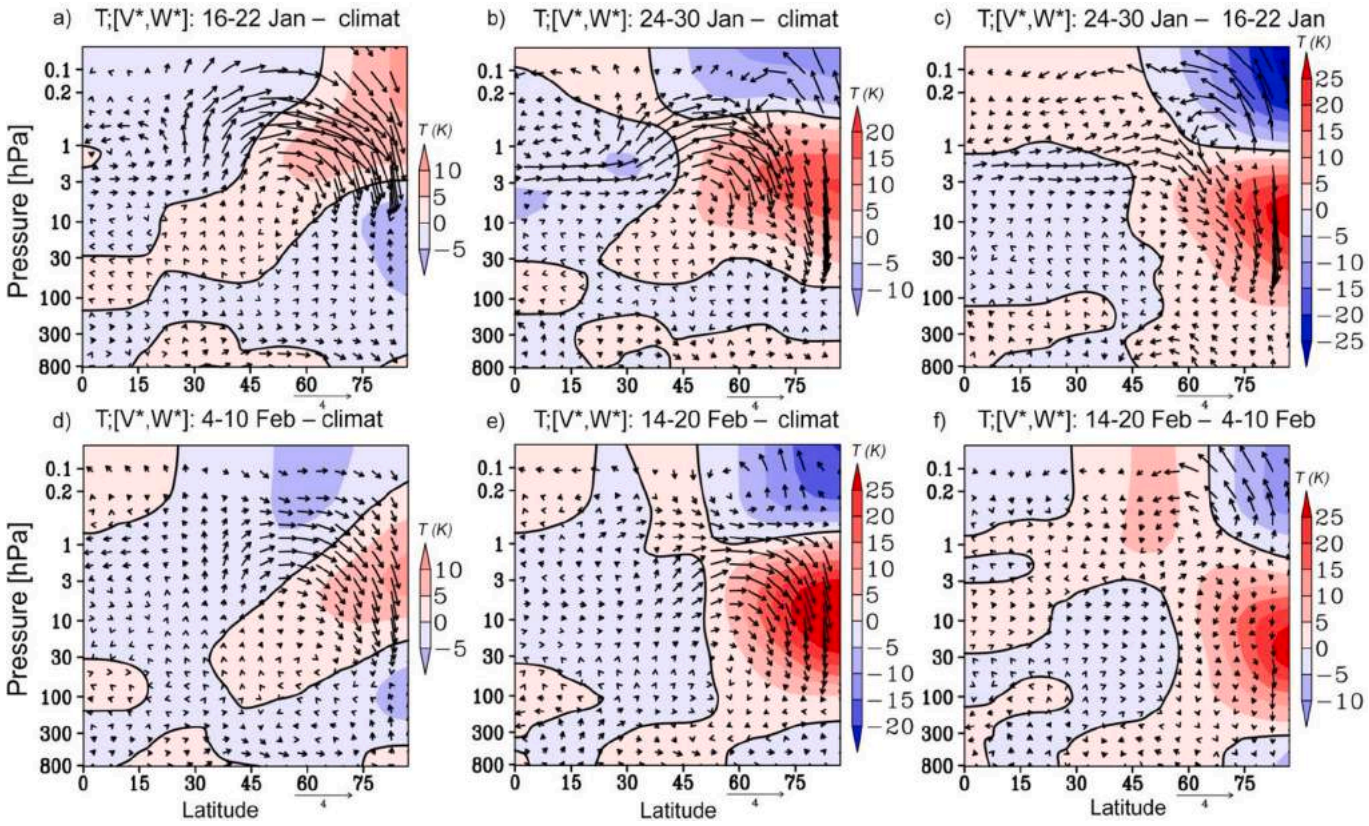

Fig. 4. Altitude-latitude distributions of anomalies of the meridional V^* and vertical W^* components of the residual meridional circulation (m/s, vectors) and temperature (K, shading) from January 16 to 22 (a), from January 24 to 30, 2023 (b), from 4 to 10 February (d) and from 14 to 20 February (e) relative to the climatic values (from 2004 to 2023); differences between the intervals 24–30 and 16–22 January (c) and 14–20 and 14–20 February (f). W^* values are multiplied by 200.

Southeastern Siberia, Mongolia and Northeastern China in the region of 40° N - 60° N and ~ 120° E - 150° E (Fig. 5d, e), where the maximum of the upward propagation of wave activity is usually observed in winter (e.g., Zyulyaeva and Zhadin, 2009; Wei et al., 2021; Gečaitė, 2021). The intensification of the cyclone (characterized by negative deviation of geopotntial heights from zonal mean) over this region, in late January was accompanied by an increase in the upward wave activity propagation into the stratosphere with a maximum at the western periphery of this cyclone (Fig. 5 g, h, i).

Part of the wave activity due to reflection in the upper stratosphere was redirected to the lower stratosphere and troposphere above Canada as it is evidenced by the negative values of the vertical component of the Plumb vectors *Fz* in the lower stratosphere at 50 hPa in this region (Fig. 5e and f). The strengthening of cyclone in troposphere and lower stratosphere over Northeastern Eurasia at the end of January is illustrated in Fig. 5j.

The reflection of wave activity in the upper stratosphere during the minor SSW at the end of January is also confirmed by the first negative values of the reflection index for the winter season (Fig. 6j). Similar diagrams for the periods January 20–22, January 24–26, and January 30–February 1 are presented in the Appendix C (Fig. B11). They also illustrate the main features of wave activity propagation including its downward propagation over Canada in late January - early February described above.

In early February a slightly weakening of the wave activity fluxes propagating to the stratosphere and a strengthening of zonal wind were observed (Fig. 5c, f), but the reflection of wave activity fluxes into the troposphere over Canada remained (Fig. 5f). Also two additional areas of wave activity propagation appeared: upward over the Northern Europe and downward over North of Siberia nearby 60° E (Fig. 5i).

3.5. Major SSW in the middle of February 2023

The major SSW onset is connected with the intensified propagation of wave activity from the troposphere into the stratosphere with a maximum nearby 60° N (Fig. 6a, b, c). This propagation is associated with the anticyclone observed above Northwestern Europe and extended to the lower stratosphere. The strengthening of this anticyclone began in early February.

This strengthening of wave activity propagation in mid-February appears to be related to its preceding reflection from the stratosphere to the troposphere over Canada and the Northern USA, observed as a result of a minor SSW in late January, and its subsequent propagation into the upper troposphere eastward over the North Atlantic Ocean. This reflection is often observed in this region (e.g., Matthias and Kretschmer, 2020; Vargin and Kiryushov, 2019; Vargin et al., 2021; Wei et al., 2021) and is explained by the fact that the zonal wind speed in the upper stratosphere of high latitudes weakens stronger than in the middle stratosphere as a result of the minor SSW. This is shown in Fig. 6j as the negative values of the reflective index.

The analysis of the altitudinal and longitudinal components of the Plumb flux and deviations of geopotential height from zonal mean values in the area of 50° N - 70° N for 3-day periods indicates the intensification of the anticyclone in the Northwest of Europe in the middle of February. This anticyclone strengthening is accompanied by upward wave activity propagation from the troposphere to the stratosphere resulted in the major SSW (Fig. 6g, h, i). Similar diagrams for the February 1–3, 5–7, and 8–10, 2023 are posted in the Appendix D (Fig. C12). They also illustrate the main features of wave activity propagation including its eastward propagation in the upper troposphere over the North Atlantic Ocean and the anticyclone intensification

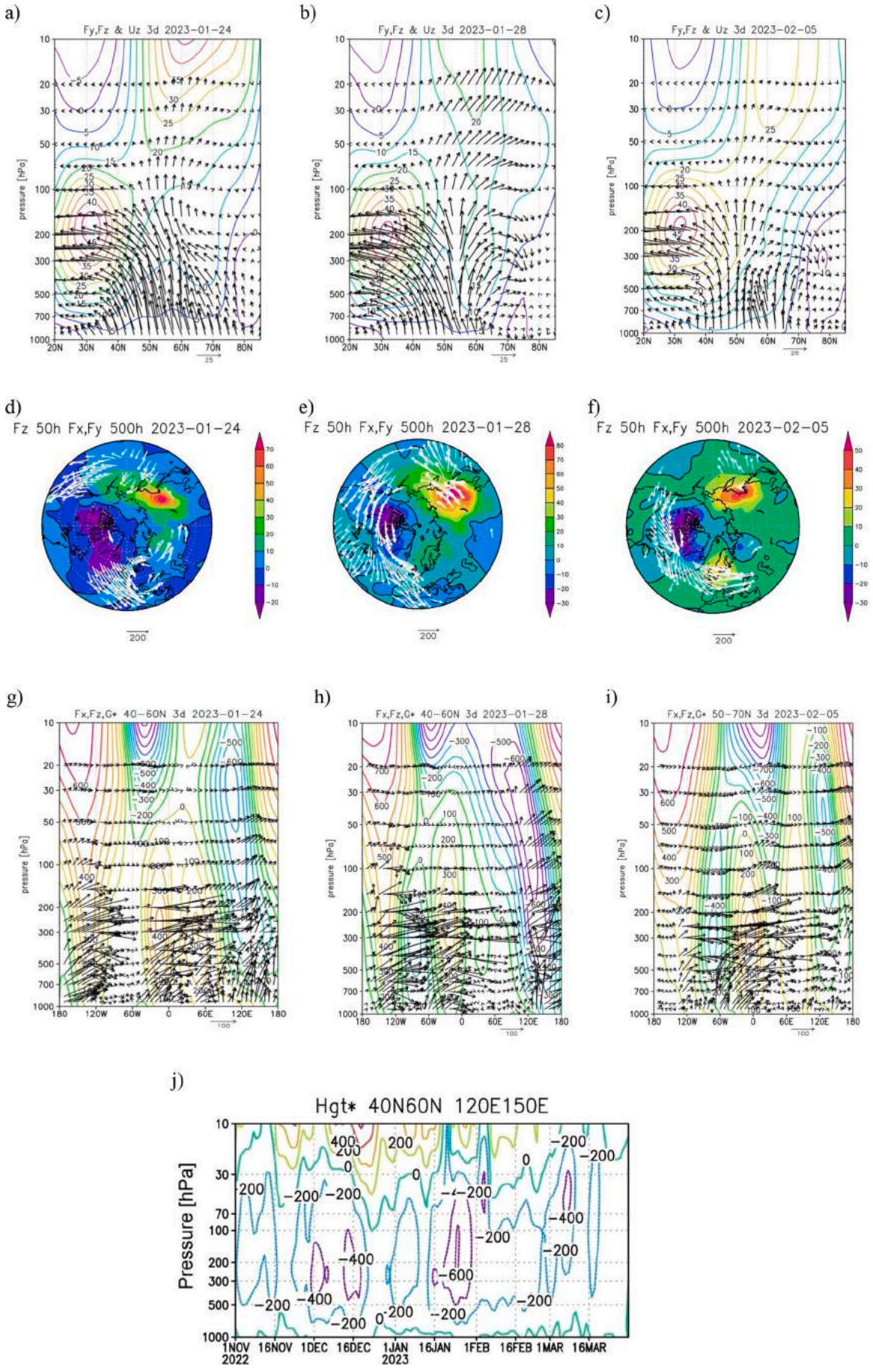

(caption on next page)

Fig. 5. Altitude - latitudinal distributions of the Plumb flux components *Fy, Fz* (m^2/s^2, arrows) and zonal mean zonal wind (m/s, contours) over the time intervals of January 22–24, January 26–28, February 3–5, 2023 (a, b, c); vertical component of the Plumb flux *Fz* at 50 hPa (shading) and *Fx, Fy* components at 500 hPa (d, e, f); altitude - longitudinal distribution of the Plumb flux components *Fx, Fz* (m^2/s^2) and geopotential height deviation from zonal mean (gpm, contours) averaged over 50° N - 70° N (g, h, i) for the same time intervals. Values of vertical component *Fz* are multiplied by 100. Height-time diagram of geopotential height deviation from zonal mean values (gpm) averaged over 40° N -60° N and 120° E − 150° E from November 1, 2022 to 30 March 2023 (j).

over the Northwestern Europe in mid-February described above.

The negative values of the reflective index corresponding to the conditions favorable for the reflection of wave activity to the lower stratosphere, except the minor SSW period at the end of January, are observed for several days during the major SSW in the middle of February and are 2 times greater by absolute value (Fig. 6j). However, in the lower stratosphere, the negative *Fz* values during the major SSW are smaller in absolute magnitude and their areas were more blurred (Fig. 6d, e, f) in comparison with the minor SSW (Fig. 5d, e, f).

The obtained evidences of the reflection of the wave activity fluxes over Canada, its subsequent propagation in the upper troposphere eastward over the North Atlantic and the associated intensification of the anticyclone over Europe cannot be considered as the only mechanism responsible for the major SSW onset in mid-February 2023, but as one of the processes that contributed to its formation.

Earlier it was shown that Rossby wave trains propagating eastward in the upper troposphere might contribute to strengthening of anticyclone over the Northern Atlantic that in turn led to enhanced upward wave activity propagation followed by a splitting of polar vortex as a result of SSW in January 2003 (Peters et al., 2010) and in January 2013 (Vargin and Medvedeva, 2015). Similar mechanism was revealed for the unique major SSW in Antarctica in September 2002 (Nishii and Nakamura, 2004; Peters et al., 2007) and verified by modeling experiments (Peters and Vargin, 2015).

3.6. Stratopause displacement

We know that in the winter hemisphere stratopause is formed due to adiabatic heating of descending air masses associated with the RMC mesospheric branch while in the summer hemisphere its formation is caused primarily by an absorption of UV radiation by ozone (Hitchman et al., 1989). In the Arctic winter seasons during the SSW onset and the next few weeks a cooling in the mesosphere temperature by tens of degrees and a stratopause height lowering are observed. These changes in turn are related to changes in the gravity waves propagation caused by zonal circulation and planetary wave propagation changes as a result of the SSW (Zulicke and Becker, 2013; Scheffler et al., 2022).

Changes in the polar upper stratosphere and mesosphere temperature affect their gas composition. For instance, the strong major SSW in January 2009 resulted in a lowering of nitrogen oxides NOx and carbon monoxide CO from the upper to lower mesosphere and into the upper stratosphere (Funke et al., 2017). The rate of chemical reactions, including those responsible for ozone formation, are also influenced by the upper stratosphere temperature changes.

According to results of observational and modeling studies, "Elevated Stratopause Event" (ESE) is mostly observed after major SSWs with a prolonged wind reversal in the lower stratosphere (Scheffler et al., 2022 and references herein). Deformation of the stratopause during ESE may be accompanied by a stronger downward transport of mesospheric air, characterized by low concentrations in water vapor (H_2O) and high concentrations in nitrous oxides ($NO_x = NO + NO_2$) and carbon monoxide (CO), into the re- established stratospheric polar vortex (e.g., Orsolini et al., 2017).

Analysis of MLS data showed that during the minor and major SSWs a long-lasting stratopause disturbance occurred at high latitudes: from the late January its height decrease, then weakening and recovery occurs in the middle of March (Fig. 7). From mid-January, a downward displacement of the region of highest temperatures characterizing the stratopause, with maxima ranging from 0.3 hPa −0.1 hPa (~57–64 km) to 3 hPa −1 hPa (~40–48 km) was observed. Simultaneously, the maximum stratopause temperature decreased from ~260 K to ~230 K until about February 10. On February 11–16, during the major SSW onset, a short-term "lowered" maximum with a temperature of ~250 K near the pressure level of 5 hPa (~37 km) was formed in the upper stratosphere. After the major SSW, the temperature of the "ordinary" stratopause decreased to ~220 K - 230 K. Simultaneously, a narrow layer of the "temporary" stratopause near 1 hPa with the maximum temperature of ~230 K was formed. The stratopause recovery was observed in late March between pressure levels ~1 hPa ando ~0.1 hPa (~48 - ~64 km) with maximum temperature up to 250 K.

The intensification of descending flows during the minor SSW in late January 2023 in the Arctic upper stratosphere in the pressure level range from ~5 hPa to ~1 hPa (~ 37–48 km), to which the stratopause has lowered, can be seen in Fig. 4b. The temperature decrease by ~10 K after the major SSW in the upper stratosphere in mid-February compared to its beginning corresponds to the intensification of ascending flows above the pressure level of 1 hPa (Fig. 4f).

3.7. SSW influence on the troposphere

It is known that Northern Annular Mode (NAM), characterized by almost longitudinally uniform structure, describes >20% of the pressure variability in the polar region from the surface to the middle stratosphere (Baldwin and Dunkerton, 1999). The interannual variability of this mode is thought to be determined by changes in the Arctic stratosphere propagating to the troposphere (Baldwin and Dunkerton, 1999; Black, 2002).

To assess the propagation of stratospheric circulation anomalies into the troposphere, the NAM index was calculated. Continuous propagation of positive anomalies of calculated NAM index (corresponding to a strong stratospheric polar vortex) from the middle stratosphere to the lower stratosphere and further to the troposphere was shortly observed in late December 2022 - early January 2023 (Fig. 8a). However, the values of anomalies were <1 sigma (σ). During this period, there was a short-term increase of the AO index from low values of −4 …-3 to close to zero values (Fig. 8b).

A continuous propagation of negative anomalies (corresponding to the weakened stratospheric polar vortex) from the middle stratosphere to the lower stratosphere and to the troposphere reaching the values of −1.5 σ was observed at the beginning of March 2023. From the end of February and during the first days of March, the AO index sharply decreased from ~3 to ~ −2. This period was characterized by the negative surface temperature anomalies in the North of Eurasia, including Northern Europe (Fig. 8c and d). A significant and prolonged cooling following the major SSW event over a large area of North America in March 2023 was reported by Lu et al. (2023).

3.8. SSW impact on ozone layer and ozone mini hole formation

Winter seasons with enhanced wave activity propagation into the stratosphere, weakened stratospheric polar vortex caused by SSW, strengthened RMC, and increased polar lower stratosphere temperature are characterized by a higher ozone content in Arctic (e.g., De La Cámara et al., 2018). As noted above, the both SSW events led to decrease of PSC NAT volume to nearly zero, which did not recover till the end of the winter season. Therefore, a strong ozone layer destruction in the lower stratosphere was not observed. As a result of the major SSW, the minimum temperature of the polar lower stratosphere increased by ~10 K,

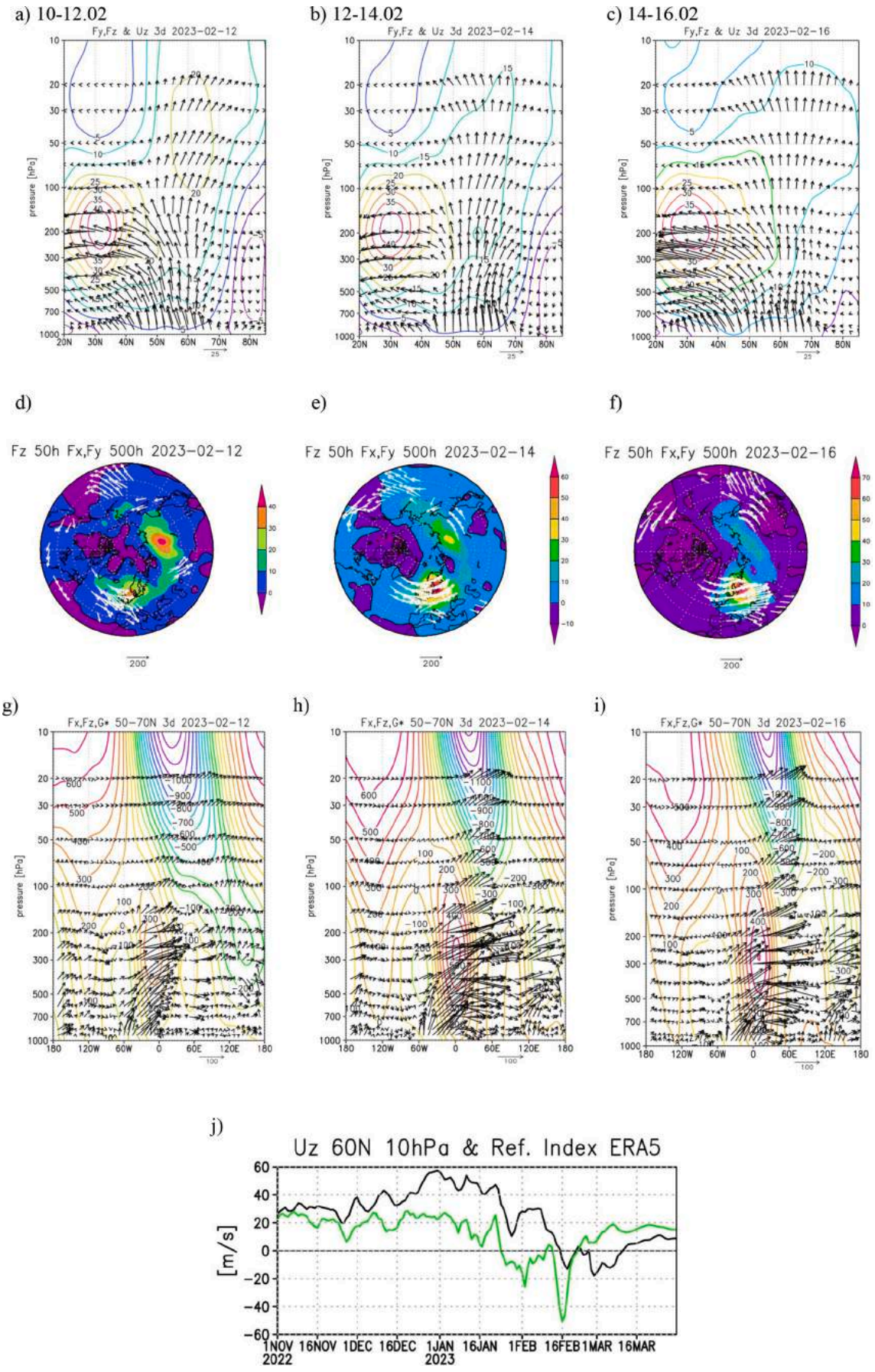

(caption on next page)

Fig. 6. Altitude - latitudinal distribution of the Plumb flux components *Fy, Fz* (m^2/s^2, vectors) and zonal mean zonal wind (m/s, contours) during time intervals of February 10–12, 12–14, and 14–16 (a, b, c). Plumb flux vertical component *Fz* at 50 hPa (contours) and *Fx, Fy* components at 500 hPa (d, e, f); altitude - longitudinal distributions of the Plumb flux components *Fx, Fz* and geopotential height deviation from zonal mean (gpm, contours) averaged over 50° N - 70° N for the same time intervals (g, h, i). Values of *Fz* component are multiplied by 100. Zonal mean zonal wind at 10 hPa and 60° N (black curve) and reflective index (green curve) (j). (For interpretation of the references to colour in this figure legend, the reader is referred to the web version of this article.)

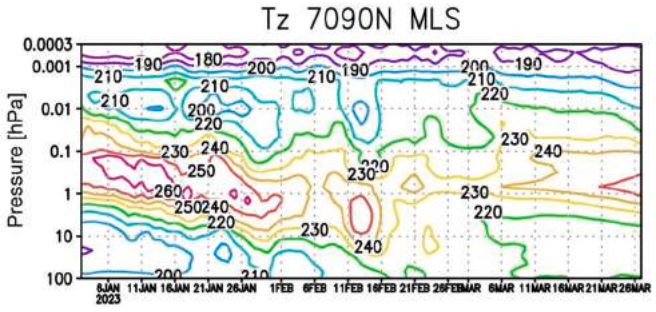

Fig. 7. Zonal mean temperature (K) averaged over 70° N - 90° N in the range of pressure levels from 100 hPa to 0.0003 hPa (~16 km - ~105 km) in January–March 2023 according to MLS data.

reaching the climatic values by the end of February, and in early March it was ~10 K higher.

Increased temperature of the Arctic lower stratosphere, caused by the both SSW events, led to the total ozone content (TOC) being close to the climatic values in March 2023 (Fig. 9a). For comparison, in March 2020 in the coldest winter season with a stable stratospheric polar vortex and record ozone loss over all years of observations, the negative TOC anomalies reached up to 150 Dobson units (DU) (Fig. 9b).

An interesting peculiarity of the onset period of the major SSW was the formation of an area of decreased TOC values or ozone mini hole (OMH) over Northern and Central Europe on February 12–16 (Mukhtarov et al., 2023; Ivanova et al., 2023). The minimum TOC values were recorded over Southern Norway and Sweden, Denmark, Northern Germany, Poland and were up to ~230 DU, which is ~40% less than the climatic values from the ground and satellite observations archived in the *Canadian Centre for Environment and Climate* (2024). The region of decreased TOC values associated with this OMH expanded to the South, resulting in TOC decrease, for example, near the Bulgarian capital Sofia (42° N, 24° E) to ~250 DU according to ground-based observations (Mukhtarov et al., 2023).

The formation of OMH is mainly determined by dynamic mechanisms and connected with the increase of the tropopause height at the passage of anticyclones (Peters et al., 1995; James, 1998). In some cases, in the formation of OMH in the winter-spring period, as, for example, in the North of Siberia in January–March 2016, a heterogeneous reactions contribute to the ozone destruction in the lower stratosphere (Timofeyev et al., 2018; Sitnov and Mokhov, 2021). The calculations showed that

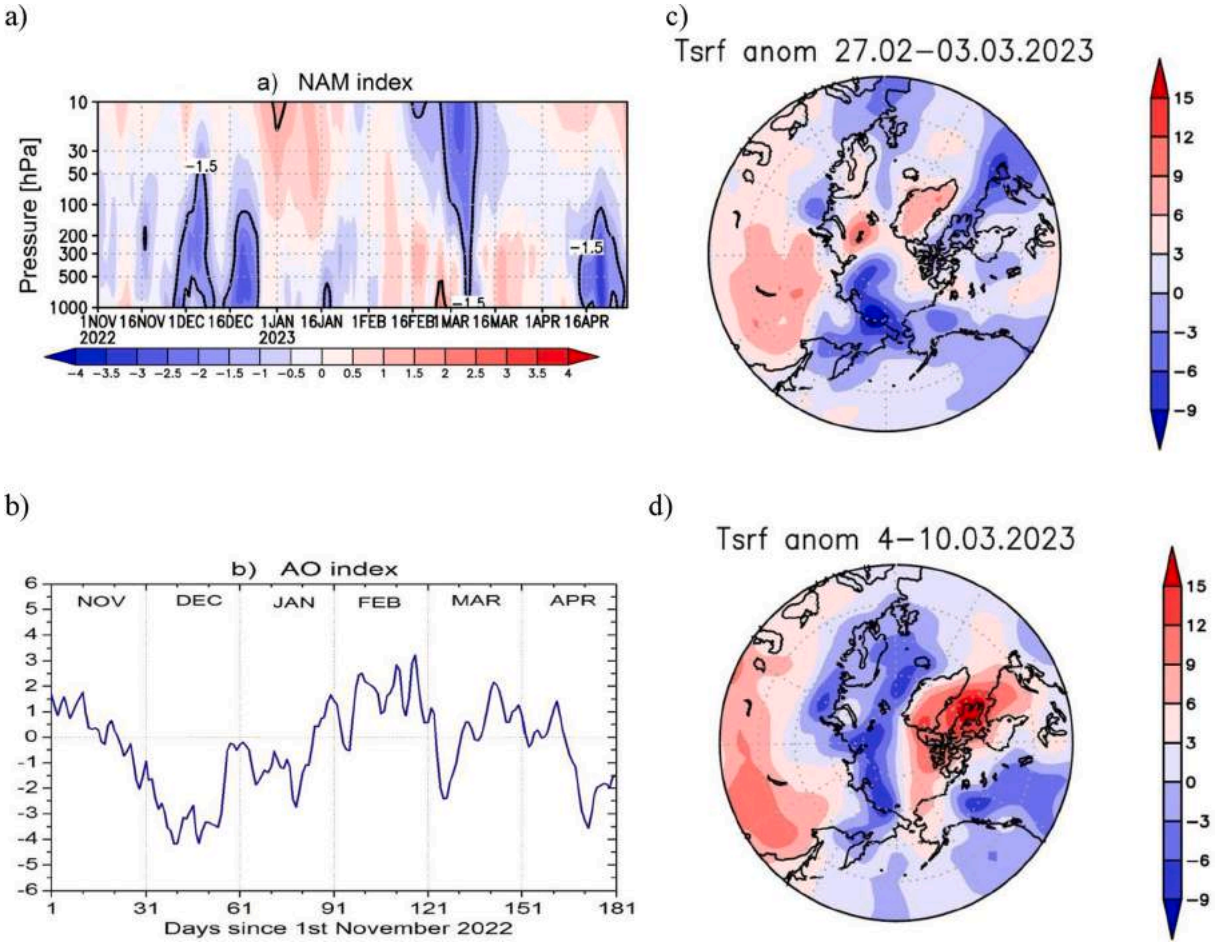

Fig. 8. Northern annular mode (NAM) index. Black solid contour line indicates +/− 1.5 σ (standard deviation) (a). Arctic oscillation (AO) index (b) from November 2022 to April 2023. Surface temperature anomalies (K) over February 27–March 3 and March 4–10, 2023 respective to climate mean (c, d).

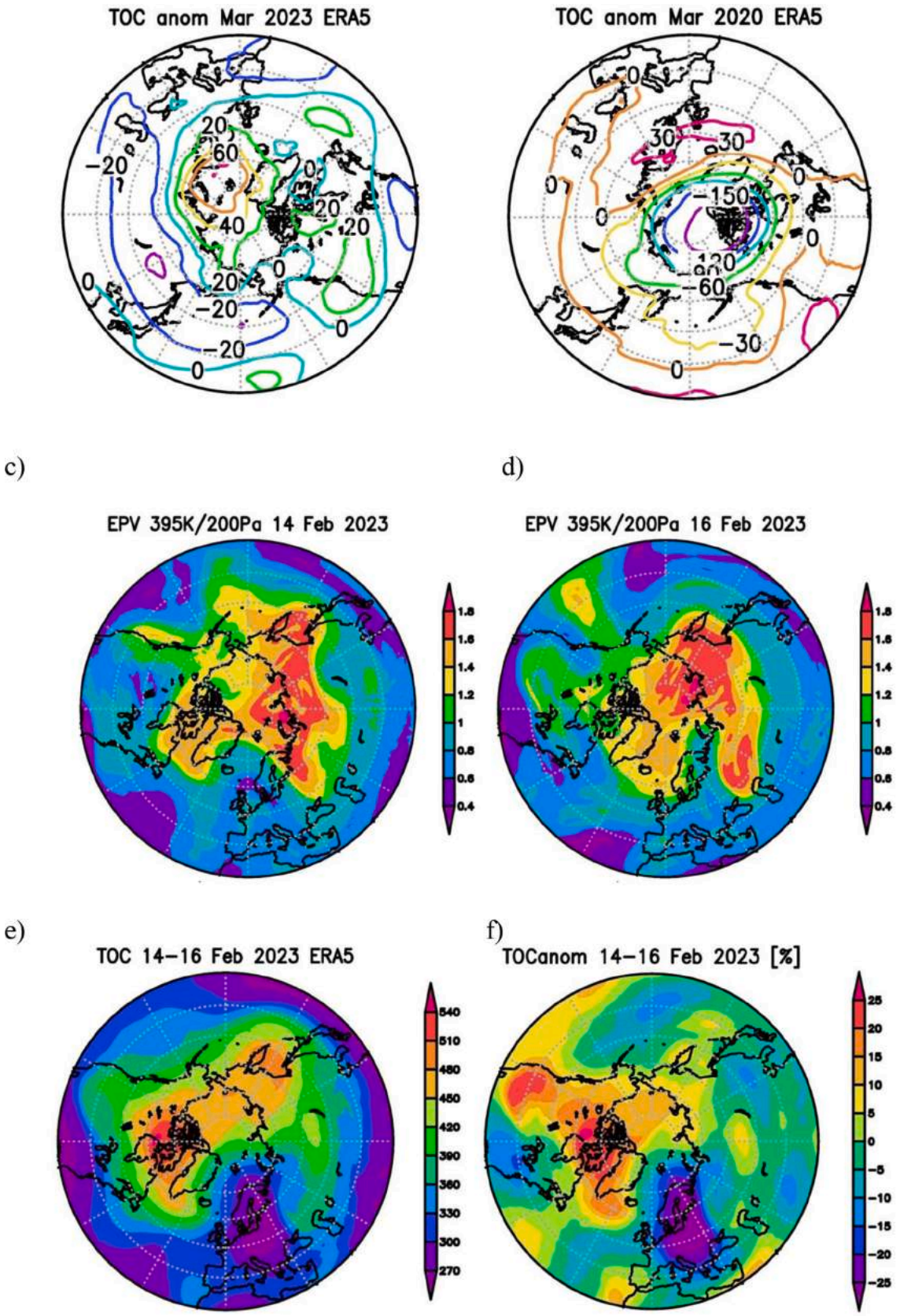

Fig. 9. Total column ozone monthly mean anomalies (DU) in March 2023 and March 2020 relative to climate mean from 1979 to 2010 (a, b). Ertel potential vorticity (10^{-3} PVU, 1 PVU = 10^{-6} K m^{-2} s^{-1} kg^{-1}) in the lower stratosphere at the isentropic level of 395 K (~200 hPa) on February 14 and February 16, 2023 (c, d). Total column ozone and its anomalies (%) from climate mean over February 14–16, 2023 (e, f).

the TOC decrease associated with this OMH in January–March 2016 did not have a significant effect on the surface UV radiation (Chubarova et al., 2019). However, in late spring of 2021 at lower latitudes, even smaller reductions in the TOC could lead to an increase in the level of erythemal UV radiation to the values that pose a risk to human health (Vargin et al., 2023).

It is assumed that the formation of the OMH over Northern and Eastern Europe in February 2023 was associated with the strengthening of the anticyclone and the accompanying tropopause elevation, which resulted in the decrease of ozone content in the lower stratosphere. Additionally, the transport of low ozone air masses from the subtropics northward along the western periphery of the anticyclone is resulted in the substitution of ozone-rich air near the maximum TOC at high latitudes.

Maps of the Ertel potential vorticity (EPV) in the lower stratosphere at the isentropic level of 395 K (~200 hPa) show the distribution of decreased EPV values over Northern - Central Europe on February 14–16 (Fig. 9 c, d). Such redistribution of EPV corresponds to the Rossby wave breaking of the anticyclonic type. When averaging for February 14–16, the minimum TOC values inside the OMH over Europe were 270 DU, and the negative anomalies were up to 25% according to the ERA5 reanalysis data (Fig. 9 e, f).

4. Discussion and conclusions

This paper examines the circulation of the Arctic stratosphere in the winter of 2022–2023 characterized by the minor and major SSW events in January–February. For this purpose, on the basis of reanalyses of meteorological information, the parameters of the large-scale dynamical processes, including components of the global meridional circulation and wave activity fluxes were analyzed. As interannual variability of Arctic winter stratosphere dynamics remains as a challenge to researchers the detailed analysis of stratosphere - troposphere dynamical coupling during highly disturbed Arctic stratosphere winter 2022–2023 with two minor SSW events and the following major one is of interest and can be useful particularly to an improvement of seasonal forecast systems.

The 2022–2023 winter season was an example of a strong intra-seasonal variability of the Arctic stratosphere: the strong and cold polar vortex at the beginning of winter with the polar lower stratosphere temperatures comparable to those in the 2019–2020 winter, when the most stable and longest-lasting polar vortex was observed, weakened by mid-January 2023, followed by the formation of a minor but strong SSW event at the end of January. Despite the fact that minor SSWs usually occur more often than major ones, as a rule they do not introduce significant disturbances into the lower polar stratosphere, unlike the event observed in January 2023. Global circulation from the lower to the upper stratosphere was strongly influenced by this minor SSW. After the minor SSW, a partial restoration of circulation occurred within a week and a major SSW was formed in mid-February. Both SSW events were accompanied by a record enhanced wave activity propagation from troposphere into the stratosphere in January–February 2023 over recent decades that is distinguishing feature of the analyzed winter season that was not addressed previously.

The minor SSW and the major SSW with a long-lasting impact on middle - lower polar stratosphere prevented ozone layer depletion. As a result, the total ozone content in the Arctic in March 2023 was close to climatic values with positive anomalies of up to ~60 DU.

After the minor and major SSW events, a prolonged disruption of the stratopause was observed at high northern latitudes: descent during the minor SSW onset in late January, then cooling by about 20 K with subsequent warming in the mid-February lasted around a week and slowly decent of newly-built stratopause from the lower mesospheric heights (“Elevated Stratopause Event” or ESE) to its climatological height in late February and warming to pre-SSW values of about 250 K in late March. This ESE occurred after long-lasting zonal wind reversal caused by the major SSW.

Results of our analysis revealed a mechanism of OMH formation over Northern - Central Europe after the SSW in February 2023: strengthening of anticyclone accompanied by tropopause elevation, which resulted in the decrease of ozone content in the lower stratosphere and the northward transport of low ozone air masses from the subtropics along the western periphery of the anticyclone. The strengthening of anticyclone was caused by Rossby wave breaking event that is was clearly seen on the Ertel potential vorticity (EPV) maps. Our result complements a relationship between TOC and temperature changes in the lower stratosphere nearby the altitude of ozone concentration maximums related to the major SSW in February 2023 revealed by (Mukhtarov et al., 2023) that also contributed to the OMH formation. However, as OMHs rather often appeared in extratropical latitudes during the winter season (Millán and Manney, 2017) the roles of both factors in this OMH formation can be estimated only with numerical modeling experiments that are beyond the scope of the present study.

Overall the main obtained results of our study can be summarized as follows:

1. In December 2022 and the first half of January 2023, a strong and persistent Arctic stratospheric polar vortex was formed. The process of strengthening the vortex was caused by a weakening of the wave activity of planetary waves. The isolation of the polar vortex at this time contributed to the cooling of the lower polar stratosphere to its minimum values for all years of observations.
2. The weakening of the stratospheric polar vortex in mid-January was accompanied by increased wave activity propagation. The lower stratosphere temperature increased by ~20 K by the end of January and led to a sharp decrease in Vpsc. Further, as a result of the burst of the planetary wave activity propagation the major SSW event was formed on February 16, which led to the reversal of the mean zonal wind in the middle stratosphere persisted until March 10.
3. The propagation of wave activity from troposphere to stratosphere in January – February 2023 was the strongest over recent decades since 1948 that resulted in increased Arctic stratospheric temperature during the middle and late winter and prevented severe ozone depletion in spring.
4. Analysis of the RMC showed that although temperature anomalies in the polar region during the major SSW in mid-February were greater than those during the minor SSW in late January, the enhancement of the RMC was stronger during the minor SSW. In general, the minor SSW was accompanied by more substantial changes in the dynamic parameters, including changes in wave activity fluxes compared to the major SSW.
5. In late January, increased reflection of wave activity from the stratosphere into the troposphere was distinguished over Canada and the Northern United States. This reflection was due to a decrease in zonal wind in the upper stratosphere associated with the minor SSW. This SSW was followed by the eastward propagation of wave activity in the upper troposphere over the North Atlantic. As a result, significant increase in wave activity propagation into the stratosphere over Northwestern Europe occurred, which caused the formation of a major SSW in mid-February. This contribution of wave activity propagation changes associated with the minor SSW to the following major SSW formation is remarkable and needs further investigations.
6. The strengthening of anticyclone led to an increase in the tropopause height and contributed to the formation of OMH over Northern and Central Europe in mid-February additionally to related to the major SSW temperature changes affected the ozone concentration in the lower stratosphere nearby its maximum.

Finally, this study is intended to expand our understanding of the mechanisms responsible for the interseasonal and interannual variability of dynamic processes in the winter Arctic stratosphere focusing on the winter 2022–2023. This variability can influence not only the

circulation of the middle atmosphere and ozone layer, but also spread into the lower atmosphere, influencing weather conditions. However, despite decades of research, many aspects of this variability are still unclear. Therefore, the further development of SSW forecasting and monitoring needs to take into account detailed analysis of every single SSW event in order to broaden statistics and systematics of atmospheric dynamic processes associated with it. Further investigation of the causes of the variability of wave activity propagation into the stratosphere is needed, including model experiments taking into account possible impacts of external factors, such as La Niña, Madden-Julian oscillation, severe loss of Barents-Laptev Sea ice observed in the 2022–2023 winter.

Funding

This research was funded by the Russian Science Foundation, Grant # 20-77-10006-P.

CRediT authorship contribution statement

P.N. Vargin: Writing – review & editing, Validation, Investigation, Formal analysis, Conceptualization. **A.V. Koval**: Writing – review & editing, Validation, Investigation, Formal analysis. **V.V. Guryanov**: Investigation, Formal analysis. **B.M. Kirushov**: Investigation, Formal analysis.

Declaration of competing interest

The authors declare that they have no known competing financial interests or personal relationships that could have appeared to influence the work reported in this paper.

Data availability

Data of calculations will be provided upon request.

Acknowledgments

Following data were provided by: ERA5 reanalysis - Copernicus Climate Change Service, NCEP Reanalysis - Climate Prediction Center (NOAA), MERRA-2 reanalysis and MLS / Aura satellite - the National Aeronautics and Space Administration (NASA). Estimates of PSC I-type (NAT) volume were provided by NASA Ozone Watch project. Authors are very grateful to two unknown reviewers for their useful comments and suggestions.

Appendix A. Appendix

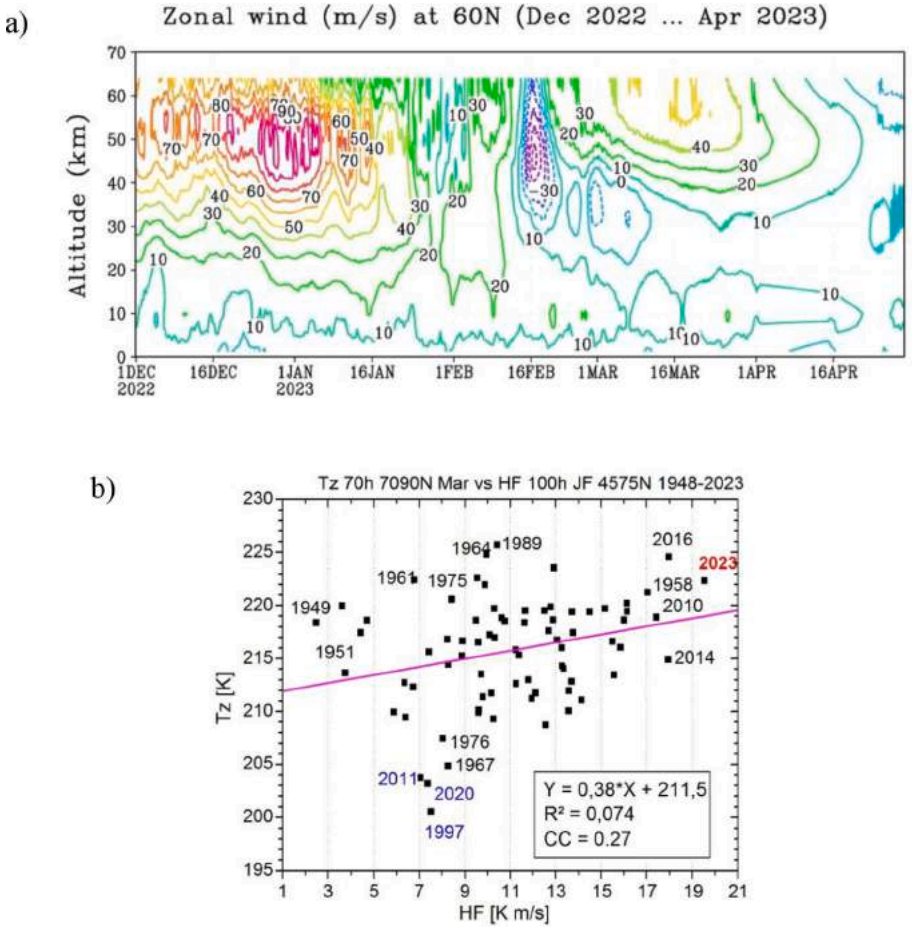

Fig. A10. Zonal mean wind at 60° N from December 1, 2022 to April 30, 2023 (a). Scatter diagram of lower stratosphere temperature mean 70° N - 90° N at 70 hPa in March vs zonal mean heat flux 45°N -75° N mean at 100 hPa in January–February from 1948 to 2023 (b). Three March months with the lowest temperature (1997, 2011, 2020) and March 2023 with the largest HF are marked by blue and red colors respectively

Appendix B

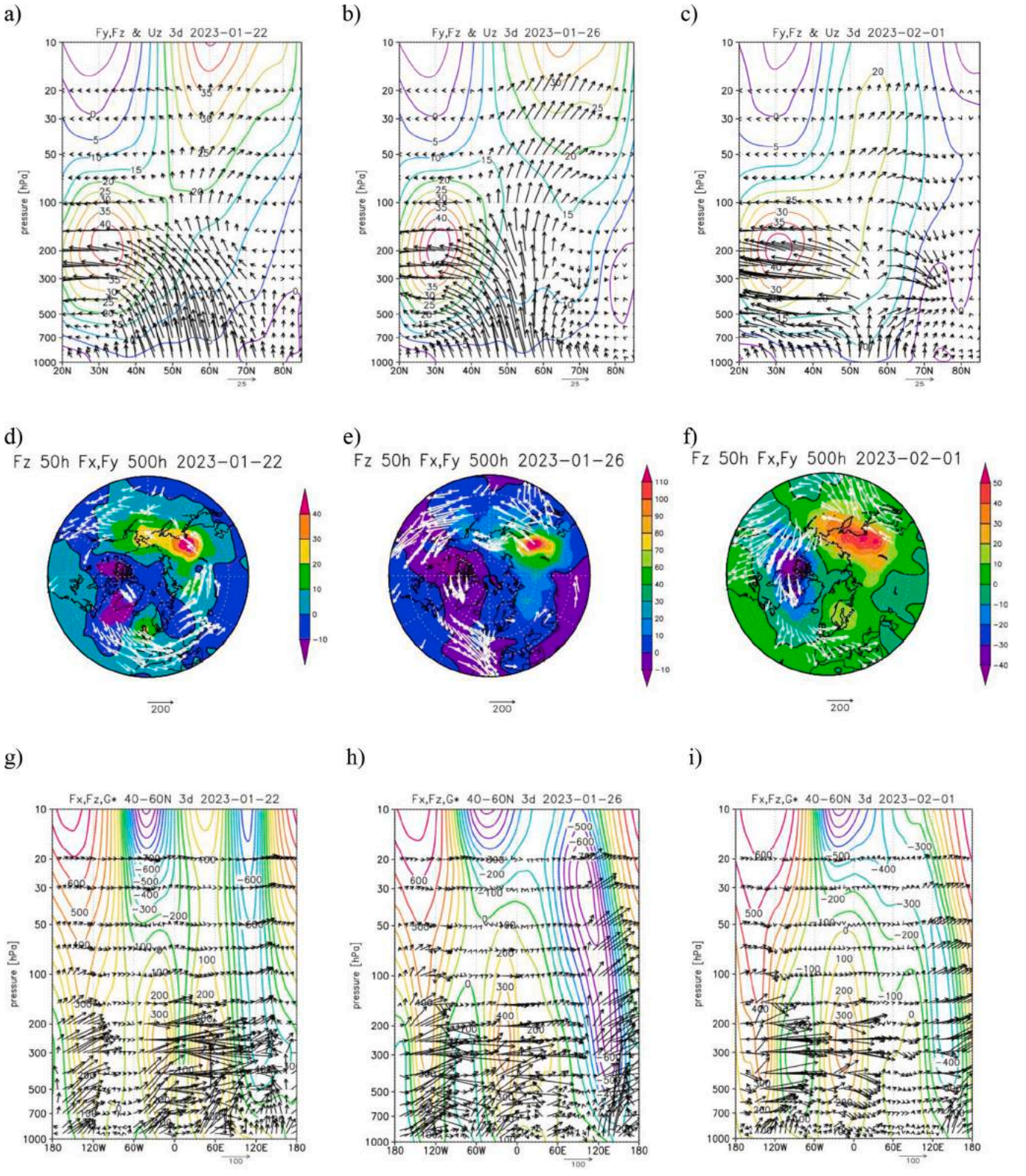

Fig. B11. Diagram of altitudinal and latitudinal Plumb flux components *Fy, Fz* (m^2/s^2) distribution and zonal mean zonal wind (m/s) (contours) over the periods of January 20–22 and January 24–26, January 30–February 1, 2023 (a, b, c), Plumb flux vertical component *Fz* at pressure level 50 hPa (contours) and *Fx, Fy* components at 500 hPa (d, e, f); diagrams of altitudinal and longitudinal Plumb flux components *Fx, Fz* [m^2/s^2] distribution and geopotential height deviation from zonal mean (gpm) (contours) averaged over 50° N - 70° N (g, h, i) for the same periods. Values of vertical component *Fz* are multiplied by 100.

Appendix C

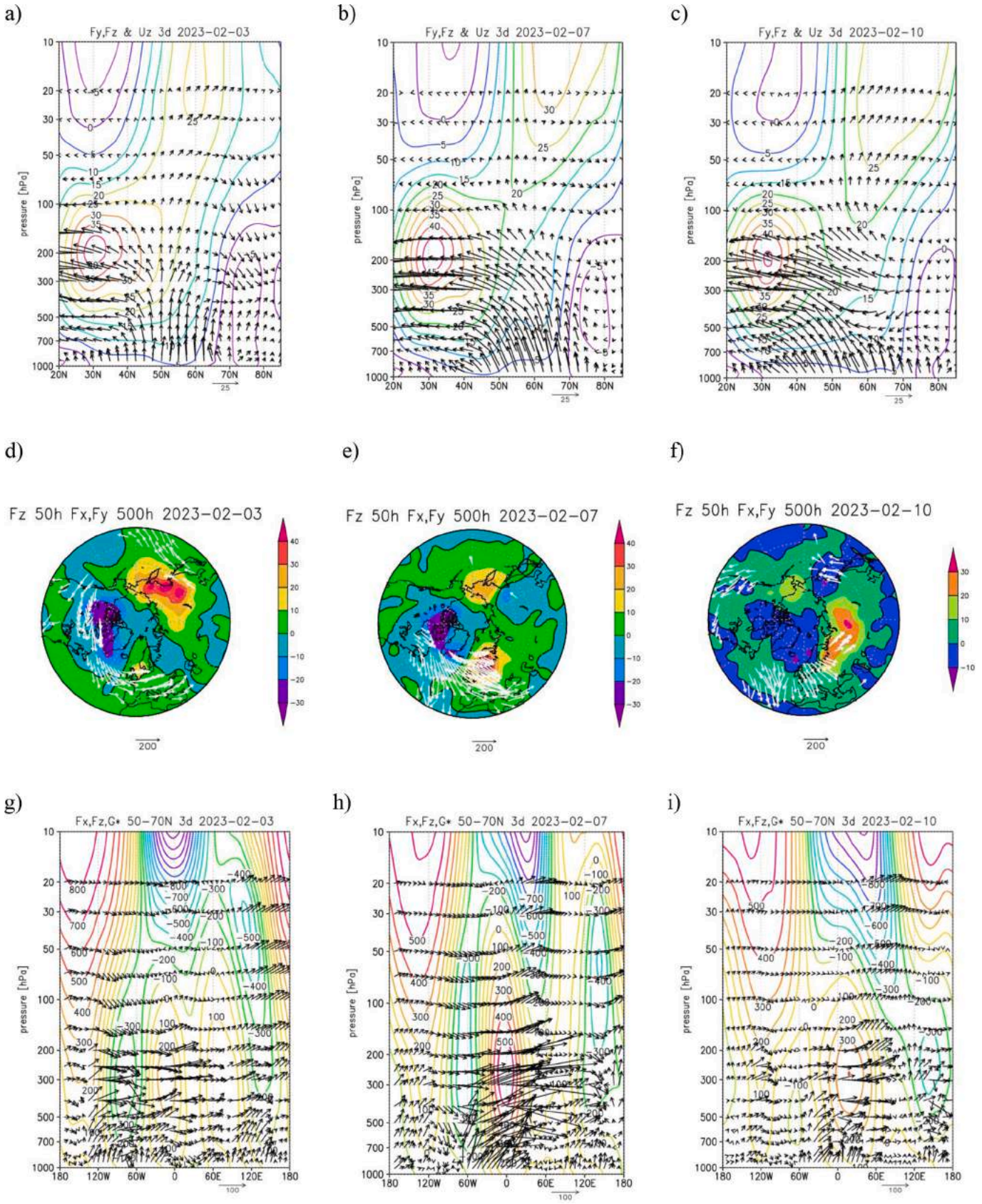

Fig. C12. Diagram of altitudinal and latitudinal Plumb flux components *Fy, Fz* (m^2/s^2) distribution and zonal mean zonal wind (m/s) (contours) over the periods of February 1–3, February 5–7, February 8–10, 2023 (a, b, c), Plumb flux vertical component *Fz* at pressure level 50 hPa (contours) and *Fx, Fy* components at 500 hPa (d, e, f); diagrams of altitudinal and longitudinal Plumb flux components *Fx, Fz* (m^2/s^2) distribution and geopotential height deviation from zonal mean (gpm)

(contours) averaged over 50° N - 70° N (g, h, i) for the same periods. Values of vertical component *Fz* are multiplied by 100.

References

Andrews, D.G., Holton, J.R., Leovy, C.B., 1987. Middle Atmosphere Dynamics. Academic Press, Orlando, Florida.

Ayarzaguena, B., Palmeiro, F., Barriopedro, D., Calvo, N., Langematz, U., Shibata, K., 2019. On the representation of major stratospheric warmings in reanalyses. Atmos. Chem. Phys. 19, 9469–9484. https://doi.org/10.5194/acp-19-9469-2019.

Baldwin, M., Dunkerton, T., 1999. Propagation of the Arctic Oscillation from the stratosphere to the troposphere. J. Geophys. Res. 104 (D24), 30937–30946.

Baldwin, M., et al., 2019. 100 years of Progress in Understanding the Stratosphere and Mesosphere. Meteorol. Monogr. 59 https://doi.org/10.1175/AMSMONOGRAPHS-D-19-0003.1, 27.1–27.61.

Baldwin, M.P., Ayarzagüena, B., Birner, T., Butchart, N., Butler, A.H., Charlton-Perez, A. J., et al., 2021. Sudden Stratospheric Warmings. Rev. Geophys. 58 https://doi.org/10.1029/2020RG000708 e2020RG000708.

Black, R.X., 2002. Stratospheric forcing of surface climate in the Arctic Oscillation. J. Clim. 15, 268–277. https://doi.org/10.1175/1520-0442(2002)015<0268:SFOSCI>2.0.CO;2.

Butchart, N., 2022. The stratosphere: a review of the dynamics and variability. Weather Clim. Dynam. 3, 1237–1272. https://doi.org/10.5194/wcd-3-1237-2022.

Butler, A.H., Seidel, D.J., Hardiman, S.C., Butchart, N., Birner, T., Match, A., 2015. Defining Sudden Stratospheric Warmings. Bull. Amer. Meteor. Soc. 96, 1913–1928. https://doi.org/10.1175/BAMS-D-13-00173.1.

Canadian Centre for Environment and Climate. https://exp-studies.tor.ec.gc.ca/cgi-bin/clf2/selectMap, 2024 accessed on March 15.

Chubarova, N.E., Timofeev, Yu.M., Virolainen, Ya A., Polyakov, A.V., 2019. Estimates of UV indices during the periods of reduced ozone content over Siberia in winter-spring 2016. Atmos. Ocean. Opt. 32 (2), 177–179. https://doi.org/10.1134/S1024856019020040.

de Fondeville, R., Wu, Z., Székely, E., Obozinski, G., Domeisen, D.I.V., 2023. Improved extended-range prediction of persistent stratospheric perturbations using machine learning. Weather Clim Dynam. 4, 287–307. https://doi.org/10.5194/wcd-4-287-2023.

De La Cámara, A., Abalos, M., Hitchcock, P., Calvo, N., Garcia, R., 2018. Response of Arctic ozone to sudden stratospheric warmings. Atmos. Chem. Phys. 18, 16499–16513. https://acp.copernicus.org/articles/18/16499/2018/.

Funke, B., Ball, W., Bender, S., Gardini, A., Lynn, Harvey V., Lambert, A., et al., 2017. HEPPA-II model–measurement intercomparison project: EPP indirect effects during the dynamically perturbed NH winter 2008–2009. Atmos. Chem. Phys. 17, 3573–3604. https://doi.org/10.5194/acp-17-3573-2017.

Gasperini, F., Jones Jr., M., Harding, B.J., Immel, T.J., 2023. Direct observational evidence of altered mesosphere lower thermosphere mean circulation from a major sudden stratospheric warming. Geophys. Res. Lett. 50 https://doi.org/10.1029/2022GL102579 e2022GL102579.

Gečaitė, I., 2021. Climatology of three-dimensional Eliassen–Palm Wave activity fluxes in the Northern Hemisphere stratosphere from 1981 to 2020. Climate 9, 124. https://doi.org/10.3390/cli9080124.

Gelaro, R., et al., 2017. The Modern-Era Retrospective Analysis for Research and applications, Version 2 (MERRA-2). J. Clim. 30, 5419–5454. https://doi.org/10.1175/JCLI-D-16-0758.1.

Goncharenko, L., Coster, A., Chau, J., Valladares, C., 2010. Impact of sudden stratospheric warmings on equatorial ionization anomaly. J. Geophys. Res. 115, A00G07. https://doi.org/10.1029/2010JA015400.

Hersbach, H., et al., 2020. The ERA5 global reanalysis 1999-2049. Q. J. R. Meteorol. Soc. 146, 1999–2049. https://doi.org/10.1002/qj.3803.

Hitchman, M.H., Gille, J.C., Rodgers, C.D., Brasseur, G., 1989. The separated polar winter stratopause - a gravity wave driven climatological feature. J. Atmos. Sci. 46, 410–422. https://doi.org/10.1175/1520-0469(1989)046 0410:TSPWSA 2.0.CO;2.

Ivanova, N.S., Kuznetsova, I.N., Lezina, E.A., 2023. Ozone Content over the Russian Federation in the first quarter of 2023. Russ. Meteorol. Hydrol. 48, 548–554. https://doi.org/10.3103/S1068373923060079.

James, P.M., 1998. A Climatology of ozone Mini-holes over the Northern Hemisphere. Int. J. Climatol. 18, 1287–1303. https://doi.org/10.1002/(SICI)1097-0088(1998100)18:12<1287::AID-JOC315>3.0.CO;2-4.

Kalnay, E., et al., 1996. The NCEP/NCAR 40-year reanalysis project. Bull. Am. Meteorol. Soc. 77, 437–470.

Karpechko, A., Charlton-Perez, A., Balmaseda, M., Tyrrell, N., Vitart, F., 2018. Predicting sudden stratospheric warming 2018 and its climate impacts with a multimodel ensemble. Geophys. Res. Lett. 45, 13,538–13,546. https://doi.org/10.1029/2018GL081091.

Klimenko, M.V., Klimenko, V.V., Bessarab, F.S., Korenkov, Yu.N., Liu, H., Goncharenko, L.P., Tolstikov, M.V., 2015. Study of the thermospheric and ionospheric response to the 2009 sudden stratospheric warming using TIME-GCM and GSM TIP models – first results. J. Geophys. Res. Space Physics 120, 7873–7888. https://doi.org/10.1002/2014JA020861.

Kodera, K., Mukougawa, H., Itoh, S., 2008. Tropospheric impact of reflected planetary waves from the stratosphere. Geophys. Res. Lett. 35, L16806. https://doi.org/10.1029/2008GL034575.

Kolstad, E., Breiteig, T., Scaife, A., 2010. The association between stratospheric weak polar vortex events and cold air outbreaks in the Northern Hemisphere. Quart. J. Roy. Meteorol. Soc. 136, 886–893. https://doi.org/10.1002/qj.620.

Koval, A.V., Chen, W., Didenko, K.A., Ermakova, T.S., Gavrilov, N.M., Pogoreltsev, A.I., et al., 2021. Modelling the residual mean meridional circulation at different stages of sudden stratospheric warming events. Ann. Geophys. 39, 357–368. https://doi.org/10.5194/angeo-39-357-2021.

Labitzke, K., 1972. Temperature changes in the mesosphere and stratosphere connected with circulation changes in winter. J. Atmos. Sci. 29, 756–766.

Lawrence, Z., Manney, G., Wargan, K., 2018. Reanalysis intercomparisons of stratospheric polar processing diagnostics. Atmos. Chem. Phys. 18, 13547–13579. https://doi.org/10.5194/acp-18-13547-2018.

Lawrence, Z., Perlwitz, J., Butler, A., Manney, G., Newman, P., Lee, S., Nash, E., 2020. The remarkably strong Arctic stratospheric polar vortex of winter 2020: links to record-breaking Arctic Oscillation and ozone loss. J. Geophys. Res. Atmos. 125 (22), 1–21. https://doi.org/10.1029/2020JD033271.

Lawrence, Z.D., Abalos, M., Ayarzagüena, B., Barriopedro, D., Butler, A.H., Calvo, N., et al., 2022. Quantifying stratospheric biases and identifying their potential sources in subseasonal forecast systems. Weather Clim. Dynam. 3, 977–1001. https://doi.org/10.5194/wcd-3-977-2022.

Li, Y., Kirchengast, G., Schwaerz, M., Yuan, Y., 2023. Monitoring sudden stratospheric warmings under climate change since 1980 based on reanalysis data verified by radio occultation. Atmos. Chem. Phys. 23, 1259–1284. https://doi.org/10.5194/acp-23-1259-2023.

Lu, Q., Rao, J., Shi, C., Ren, R., Liu, Y., Liu, S., 2023. Stratosphere-troposphere coupling during stratospheric extremes in the 2022/23 winter. Weather Climat. Extrem. 42, 100627 https://doi.org/10.1016/j.wace.2023.100627.

Manney, G.L., Krüger, K., Sabutis, J.L., Sena, S.A., Pawson, S., 2005. The remarkable 2003–2004 winter and other recent warm winters in the Arctic stratosphere since the late 1990s. J. Geophys. Res. 110, D04107. https://doi.org/10.1029/2004JD005367.

Manney, G., Lawrence, Z., Santee, M., Read, W.G., Livesey, N.J., Lambert, A., et al., 2015. A minor sudden stratospheric warming with a major impact: Transport and polar processing in the 2014/2015 Arctic winter. Geophys. Res. Lett. 42, 7808–7816. https://doi.org/10.1002/2015GL065864.

Matthias, V., Kretschmer, M., 2020. The Influence of Stratospheric Wave Reflection on north American Cold Spells. Mon. Weather Rev. 148, 1675–1690. https://doi.org/10.1175/MWR-D-19-0339.1.

Millán, L.F., Manney, G.L., 2017. An assessment of ozone mini-hole representation in reanalyses over the Northern Hemisphere. Atmos. Chem. Phys. 17, 9277–9289. https://doi.org/10.5194/acp-17-9277-2017.

Mukhtarov, P., Miloshev, N., Bojilova, R., 2023. Stratospheric Warming events in the Period January–March 2023 and their Impact on Stratospheric ozone in the Northern Hemisphere. Atmosphere 14, 1762. https://doi.org/10.3390/atmos14121762.

NASA Ozone Watch. https://ozonewatch.gsfc.nasa.gov/meteorology/temp_2022_MERRA2_NH.html, 2024 accessed on March 15.

Nath, D., Chen, W., Zelin, C., Pogoreltsev, A.I., Wei, K., 2016. Dynamics of 2013 Sudden Stratospheric Warming event and its impact on cold weather over Eurasia: Role of planetary wave reflection. Sci. Rep. 6, 24174. https://doi.org/10.1038/srep24174.

Newman, P., Nash, E., Rosenfield, J., 2001. What controls the temperature of the Arctic stratosphere during the spring? J. Geophys. Res. 106 (D17), 19999–20010. https://doi.org/10.1029/2000JD000061.

Nishii, K., Nakamura, H., 2004. Tropospheric influence on the diminished Antarctic ozone hole in September 2002. Geophys. Res. Lett. 31, L16103. https://doi.org/10.1029/2004GL019532.

Orsolini, Y.J., Limpasuvan, V., Perot, K., Espy, P.J., Hibbins, R.E., Lossow, S., 2017. Modelling the descent of nitric oxide during the elevated stratopause event of January 2013. J. Atmos. Sol. Terr. Phys. 155, 50–61. https://doi.org/10.1016/j.jastp.2017.01.006.

Perlwitz, J., Harnik, N., 2004. Downward coupling between the stratosphere and troposphere: the relative roles of wave and zonal mean processes. J. Clim. 17, 4902–4909. https://doi.org/10.1175/JCLI-3247.1.

Peters, D., Vargin, P., 2015. Impact of extratropical Rossby wave trains on planetary wave activity in the polar southern lower stratosphere in September 2002. Tellus 67A, 25875. https://doi.org/10.3402/tellusa.v67.25875.

Peters, D., Egger, J., Entzian, G., 1995. Dynamical Aspects of ozone Mini-hole Formation. Meteorog. Atmos. Phys. 55, 205–214. https://doi.org/10.1007/BF01029827.

Peters, D., Vargin, P., Körnich, H., 2007. A Study of the Zonally Asymmetric Tropospheric Forcing of the Austral Vortex Splitting during September 2002. Tellus 59A, 384–394. https://doi.org/10.1111/j.1600-0870.2007.00228.x.

Peters, D., Vargin, P., Gabriel, A., Tsvetkova, N., Yushkov, V., 2010. Tropospheric forcing of the boreal polar vortex splitting in January 2003. Ann. Geophys. 28, 1–16. https://doi.org/10.5194/angeo-28-2133-2010.

Plumb, R., 1985. On the Three-Dimensional Propagation of Stationary Waves. J. Atmos. Sci. 42, 217–229.

Pogoreltsev, A., Savenkova, E., Aniskina, O., Ermakova, T., Chen, W., Wei, K., 2015. Interannual and intraseasonal variability of stratospheric dynamics and stratosphere-troposphere coupling during northern winter. J. Atmos. Solar-Terr. Phys. 136, 187–200. https://doi.org/10.1016/j.jastp.2015.08.008.

Rao, J., Garfinkel, C.I., Chen, H., White, I.P., 2019. The 2019 New Year stratospheric sudden warming and its real-time predictions in multiple S2S models. J. Geophys. Res. Atmos. 124 https://doi.org/10.1029/2019JD030826.

Roy, R., Kuttippurath, J., 2022. The dynamical evolution of Sudden Stratospheric Warmings of the Arctic winters in the past decade 2011–2021. SN. Appl. Sci. 4 (105) https://doi.org/10.1007/s42452-022-04983-4.

Rupp, P., Spaeth, J., Garny, H., Birner, T., 2023. Enhanced polar vortex predictability following sudden stratospheric warming events. Geophys. Res. Lett. 50 e2023GL104057.

Scheffler, J., Ayarzagüena, B., Orsolini, Y., Langematz, U., 2022. Elevated stratopause events in the current and a future climate: A chemistry-climate model study. J. Atmos. Sol.-Terr. Phys. 227, 105804 https://doi.org/10.1016/j.jastp.2021.105804.

Scherhag, R., 1952. Die explosionsartigen Stratosphärenerwärmungen des Spätwinters 1951/52. Bericht. des Deutschen Wetterdienstes in der US-Zone. 6 (38), 51–63.

Sitnov, S.A., Mokhov, I.I., 2021. Relationship of the ozone mini-hole over Siberia in January 2016 to atmospheric blocking. Dokl. Earth Sci. 500, 772–776. https://doi.org/10.1134/S1028334X21090178.

Smyshlyaev, S.P., Vargin, P.N., Motsakov, M.A., 2021. Numerical modeling of ozone loss in the exceptional Arctic stratosphere winter-spring of 2020. Atmosphere 12, 1470. https://doi.org/10.3390/atmos12111470.

Solomon, S., Garcia, R., Rowland, F., Wuebbles, D., 1986. On the depletion of Antarctic ozone. Nature 321, 755–758. https://doi.org/10.1038/321755a0.

Tian, W., Huang, J., Zhang, J., Xie, F., Wang, W., Peng, Y., 2023. Role of stratospheric processes in climate change: advances and challenges. Adv. Atmos. Sci. 40, 1379–1400. https://doi.org/10.1007/s00376-023-2341-1.

Timofeyev, Y., Smyshlyaev, S., Virolainen, Y., Garkusha, A.S., Polyakov, A.V., Motsakov, M.A., Kirner, O., 2018. Case study of ozone anomalies over northern Russia in the 2015/2016 winter: measurements and numerical modeling. Ann. Geophys. 36, 1495–1505. https://doi.org/10.5194/angeo-36-1495-2018.

Tripathi, O., Baldwin, M., Charlton-Perez, A., Charron, M., Eckermann, S., Gerber, E., et al., 2015. The predictability of the extratropical stratosphere on monthly time-scales and its impact on the skill of tropospheric forecasts. Q. J. R. Meteorol. Soc. 141, 987–1003. https://doi.org/10.1002/qj.2432.

Tsvetkova, N.D., Vyzankin, A.S., Vargin, P.N., Lukyanov, A.N., Yushkov, V.A., 2020. Investigation and forecast of sudden stratospheric warming events with chemistry climate model SOCOL. In: IOP Conference Series: Earth Environ. Sci. https://doi.org/10.1088/1755-1315/606/1/012062.

Tsvetkova, N.D., Vargin, P.N., Lukyanov, A.N., Kirushov, B.M., Yushkov, V.A., Khattatov, V.U., 2021. Investigation of chemistry ozone destruction and dynamical processes in Arctic stratosphere in winter 2019-2020. Russ. Meteorol. Hydrol. 46 (9), 597–606. https://link.springer.com/article/10.3103/S1068373921090065.

Vargin, P.N., Kiryushov, B.M., 2019. Major Sudden Stratospheric Warming in the Arctic in February 2018 and its Impacts on the Troposphere, Mesosphere, and ozone Layer. Russ. Meteorol. Hydrol. 44 (2), 112–123. https://doi.org/10.3103/S1068373919020043.

Vargin, P., Medvedeva, I., 2015. Temperature and Dynamical Regimes of the Northern Hemisphere Extratropical Atmosphere during Sudden Stratospheric Warming in Winter 2012–2013. Izv. Atmos. Ocean. Phys. 51 (1), 20–38. https://doi.org/10.1134/S0001433814060176.

Vargin, P.N., Guryanov, V.V., Lukyanov, A.N., Vyzankin, A.S., 2021. Arctic stratosphere dynamical processes in the winter of 2020-2021. Izv. *Atmos. Ocean. Phys.* 57 (6), 568–580. https://link.springer.com/article/10.1134/S0001433821060098.

Vargin, P.N., Koval, A.V., Guryanov, V.V., 2022. Arctic Stratosphere Dynamical Processes in the Winter 2021–2022. Atmosphere 13, 1550. https://doi.org/10.3390/atmos13101550.

Vargin, P.N., Fomin, B.A., Semenov, V.A., 2023. Influence of ozone mini-holes over Russian territories in May 2021 and March 2022 revealed in satellite observations and simulation. Atmos. Oceanic Optics. 36 (5), 578–589. https://doi.org/10.1134/S1024856023050172.

Waters, J., Froidevaux, L., Harwood, R., et al., 2006. The Earth observing System Microwave Limb Sounder (EOS MLS) on the Aura. IEEE Trans. Geosci. Remote Sens. 44 (5), 1075–1092. http://thz.caltech.edu/siegelpapers/MLS.pdf.

Wei, K., Chen, W., Vargin, P., 2021. Longitudinal peculiarities of planetary waves-zonal flow interaction and its role in stratosphere-troposphere dynamical coupling. Clim. Dyn. 57, 2843–2862. https://doi.org/10.1007/s00382-021-05842-5.

Wohltmann, I., von der Gathen, P., Lehmann, R., Deckelmann, H., Manney, G., Davies, J., et al., 2021. Chemical evolution of the exceptional Arctic stratospheric winter 2019/2020 compared to previous Arctic and Antarctic winters. J. Geophys. Res. Atmos. 126 https://doi.org/10.1029/2020JD034356 e2020JD034356.

Zhang, Y., Yi, Y., Ren, X., et al., 2021. Statistical Characteristics and Long-Term Variations of Major Sudden Stratospheric Warming events. J. Meteorol. Res. 35, 416–427. https://doi.org/10.1007/s13351-021-0166-3.

Zulicke, Ch., Becker, E., 2013. The structure of the mesosphere during sudden stratospheric warmings in a global circulation model. J. Geophys. Res. Atmos. 118, 2255–2271. https://doi.org/10.1002/jgrd.50219.

Zyulyaeva, Y.A., Zhadin, E.A., 2009. Analysis of three-dimensional Eliassen-Palm fluxes in the lower stratosphere. Russ. Meteorol. Hydrol. 34 (8), 483–490. https://doi.org/10.3103/s106837390 9080019.

Matsuno, T., 1971. A dynamical model of sudden stratospheric warming. J. Atmos. Sci. 28, 871–883. https://doi.org/10.1175/1520-0469(1971)028<1479:ADMOTS>2.0.CO;2.